Constitutive PS1 expression inhibits myogenic differentiation

Notch is activated by the binding of its ligands, and activated Notch is then cleaved by γ-secretase to release the Notch ICD, a central step in Notch signalling. Although γ-secretase activity is dependent on PS1 function, several studies have reported that overexpression of PS1 alone does not enhance γ-secretase activity, unless in conjunction with nicastrin, Aph-1a and Pen-2 (reviewed by De Strooper, 2003; Parks and Curtis, 2007; Vetrivel et al., 2006). To investigate the effect of constitutive PS1 expression on satellite cell function, mouse *PS1* cDNA was cloned to generate *pMSCV-PS1-IRES-GFP* or *pCMV-PS1-V5*. *pMSCV-PS1-IRES-GFP* was transfected into satellite-cell-derived myoblasts, with eGFP from the *IRES-eGFP* allowing transfected cells to be readily identified (transfection efficiency was >30% for both vectors). Constitutive PS1 expression led to fewer $eGFP^+$ cells containing MyHC (8%) (Fig. 3A and quantified in 3D) or $MyoD^+$ (62%) (Fig. 3B and quantified in 3E) compared with cells transfected with control empty *pMSCV-IRES-GFP*. Constitutive expression of PS1 also significantly increased the number of $eGFP^+$ cells expressing Pax7 by approximately fourfold over parallel cultures transfected with control siRNA (Fig. 3C and quantified in 3F).

To confirm that transfection of PS1 does not act by increasing γ-secretase activity, constitutive PS1 expression was also examined in the presence of DAPT, which is a specific pharmacological inhibitor of γ-secretase activity (Lammich et al., 2002). Importantly, the effects of PS1 on increasing the number of $eGFP^+$ satellite-cell-derived myoblasts containing Pax7 protein, was not significantly altered when γ-secretase activity was inhibited (Fig. 3F). Because inhibition of γ-secretase normally results in a decrease in Pax7 expression, these observations indicate that PS1 is exerting its effect through a mechanism that is independent of γ-secretase activity. Taken together, these results clearly demonstrate that myogenic differentiation was suppressed by overexpression of PS1, but the number of cells expressing Pax7 significantly rose, via a mechanism independent of γ-secretase activity.

PS1 negatively regulates expression of MyoD through a γ-secretase-independent mechanism

To perform detailed biochemical analysis, we also used the immortalised adult post-injury-derived C2 cell line (Yaffe and Saxel, 1977). Immunocytochemistry showed that PS1 was expressed in proliferating C2C12 myoblasts (data not shown), as observed in primary satellite-cell-derived myoblasts (Fig. 1). Both siRNAs targeting PS1 effectively reduced PS1 protein levels 48 hours after transfection in C2C12 cells (Fig. 4A) and enhanced myogenic differentiation after 72 hours in differentiation medium (DM), with

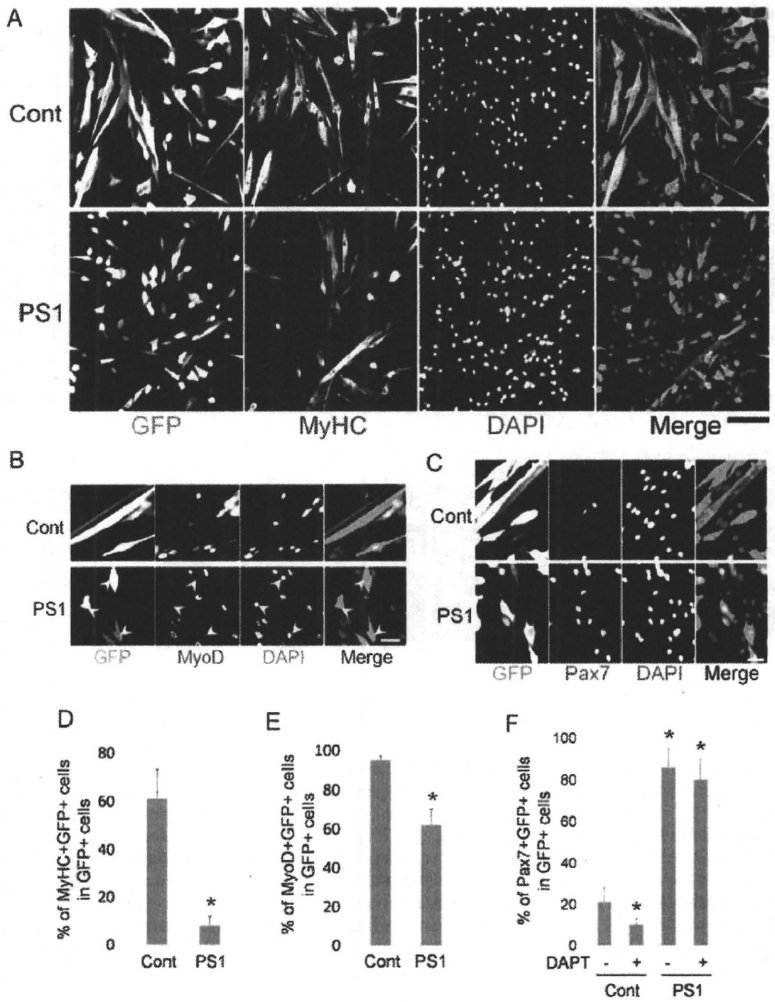

Fig. 3. Constitutive PS1 expression leads to suppression of myogenic differentiation and augmentation of Pax7 expression. The effects of PS1 on satellite cell function were examined by constitutively expressing PS1 using expression vectors. (A,B) Primary satellite-cell-derived myoblasts were transfected with either control *pMSCV-IRES-GFP* (Cont) or *pMSCV-PS1-IRES-GFP* (PS1) vectors and, 48 hours later, immunostained for eGFP (to identify transfected cells) and either MyHC (A) or MyoD (B) (arrowheads indicate GFP^+MyoD^- cells in PS1-vector-transfected cells). (D,E) Constitutive PS1 expression significantly reduced the percentage of transfected cells that co-expressed either MyHC (D), or MyoD (E). (C,F) Constitutive PS1 expression also increased the percentage of satellite-cell-derived myoblasts expressing Pax7. (F) Although exposure of control *pMSCV-IRES-GFP*-transfected cells to 1 μM DAPT reduced the percentage of Pax7-expressing cells, DAPT inhibition of γ-secretase did not prevent the significant increase of Pax7 in transfected cells containing *pMSCV-PS1-IRES-GFP* vector. Data from at least three independent experiments is shown ± s.d. Asterisks in D-F indicate that data are significantly different from control values ($P<0.05$). Scale bars: 100 μm (A) and 30 μm (B,C).

larger multinucleated myotubes formed than in control cultures (Fig. 4B). Even when maintained in growth medium (GM), transfection with either of the *PS1* siRNA species resulted in an induction of MyHC expression (Fig. 4B), though crucially, treatment with DAPT alone, to inhibit γ-secretase activity, did not result in MyHC expression (Fig. 4B). Immunblot analysis of C2C12 cells transfected with *PS1* siRNAs also revealed a lower expression of Pax7 with both duplexes than with control siRNA (Fig. 4D).

Transfection of *pMSCV-PS1-IRES-GFP* into C2C12 myoblasts resulted in high levels of PS1 and GFP protein in >70% of cells (Fig. 4E), allowing us to perform western blot analysis. As with primary satellite-cell-derived myoblasts, transfection with *pMSCV-PS1-IRES-GFP* resulted in a marked suppression of MyHC expression compared with control (Fig. 4F). Again, constitutive PS1 expression-mediated inhibition of differentiation was not influenced by the presence of DAPT to inhibit γ-secretase activity (Fig. 4G and quantified in 4H). Importantly, immunoblot analysis for Notch1 ICD, Notch2 ICD and Hes1 showed that the already-active Notch signalling in proliferating myoblasts was not further augmented by constitutive PS1 expression (Fig. 4I). Interestingly, expression of MyoD was downregulated by constitutive expression of PS1 in proliferating myoblasts, but expression of Pax7 was not affected (Fig. 4I). To check whether MyoD downregulation was influenced by γ-secretase activity, we transfected C2C12 myoblasts with *pCMV-V5-tagged PS1* in the presence of DAPT to inhibit γ-secretase activity, and found that MyoD levels still decreased significantly (Fig. 4J and quantified in 4K).

Myogenic differentiation in *PS1*-null cells is independent of γ-secretase activity

Mice homozygous for null alleles of *PS1* die late in embryogenesis (Shen et al., 1997; Wong et al., 1997), precluding examination of satellite cells. To model myogenesis in *PS1*-null cells therefore, we used ectopic MyoD expression to initiate myogenic conversion in MEFs (Skapek et al., 1996). Immunostaining revealed robust expression of PS1 in control wild-type (WT) MEFs but not $PS1^{-/-}$

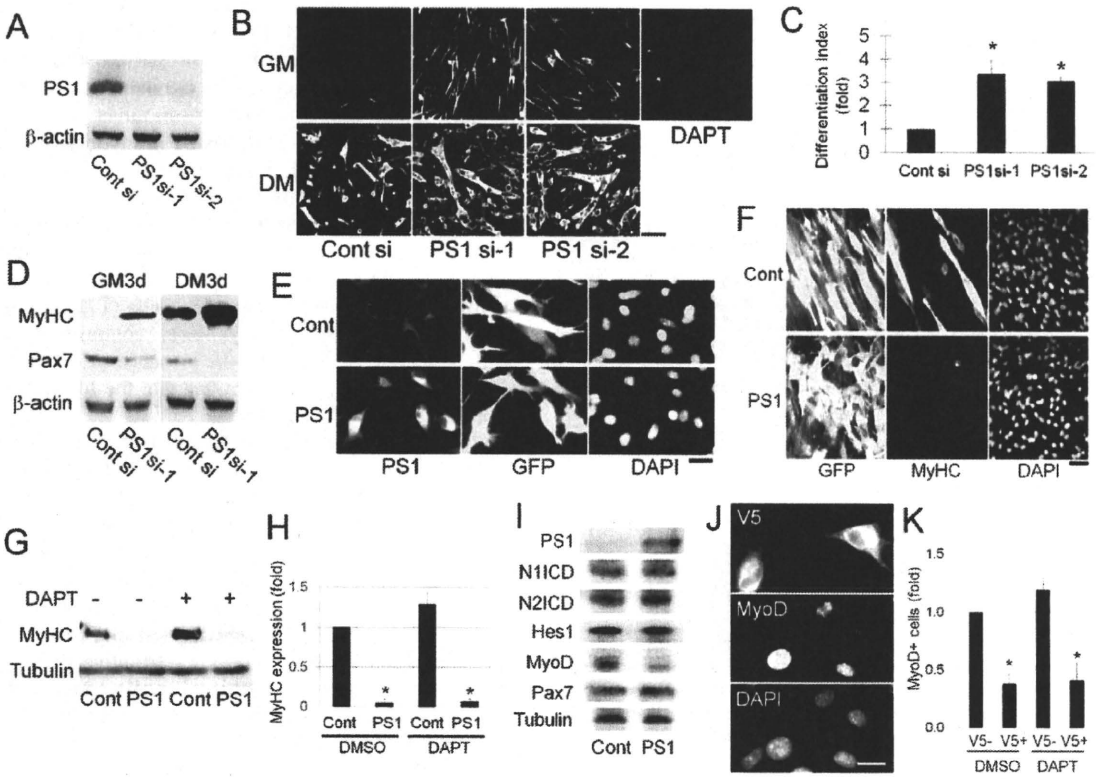

Fig. 4. PS1 negatively regulates MyoD expression in a γ-secretase-independent mechanism. In order to obtain sufficient material for biochemical analysis, we also used the adult mouse muscle-derived C2C12 myogenic cell line. (A) Immunoblot analysis showed that proliferating C2C12 cells expressed PS1, and that the siRNA-targeting PS1 (PS1si-1 and PS1si-2) was effective at reducing PS1 protein levels. (B) As with primary myoblasts, exposure of C2C12 myoblasts to siRNA against PS1 promoted myogenic differentiation, as shown by immunostaining for MyHC, in both growth (GM) and differentiation medium (DM) (quantified in C for DM). Importantly, treatment with DAPT in GM for 3 days to inhibit γ-secretase activity did not reproduce the effects of PS1 knockdown, being unable to induce expression of MyHC in C2C12 cells. (D) Immunblot analysis of siRNA-transfected C2C12 cells cultured in GM or DM for 3 days after transfection confirmed increased MyHC expression. Importantly, Pax7 levels were significantly reduced by PS1 knockdown under both culture conditions. (E-I) PS1 was also constitutively expressed in C2C12 myoblasts by transient transfection with PS1-expression vector (*pMSCV-PS1-IRES-GFP*). (F) Immunocytochemical analysis for MyHC revealed that myogenic differentiation was again inhibited. (G) Immunoblot analysis of transfected C2C12 cells constitutively expressing PS1, illustrating that inhibiting γ-secretase activity by exposure to 1 μM DAPT for 2.5 days did not alter the marked reduction in MyHC levels (quantified in H). (I) Immunoblot analysis demonstrated that constitutive PS1 expression in C2C12 cells cultured in GM for 24 hours after transfection did not affect the levels of Notch1 ICD, Notch2 ICD or Hes1, but that MyoD was significantly reduced, compared to the tubulin protein loading control. (J) Similar results were obtained using a V5-tagged PS1 expression vector transfected into C2C12 cells. Immunostaining showed that MyoD expression was reduced to a similar degree, with or without exposure to 1 μM DAPT to inhibit γ-secretase activity (quantified in K). Data from at least three independent experiments is shown ± s.d. Asterisks in C, H and K indicate that data are significantly different from control values (P<0.05). Scale bars: 100 μm (B), 20 μm (E), 30 μm (F) and 10 μm (J).

MEFs (Fig. 5A). γ-secretase activity was significant lower in *PS1*$^{-/-}$ MEFs than in control WT MEFs, as assessed using a γ-secretase activity detection kit (data not shown).

Transient transfection with a MyoD expression vector resulted in robust MyoD expression in both WT and *PS1*$^{-/-}$ MEFs (Fig. 5B). Myogenic differentiation in vitro is suppressed by culture in medium containing high levels of serum (Kodaira et al., 2006), and we observed no signs of myogenic differentiation in WT MEFs maintained in 10% FBS for 5 days after transfection with MyoD (Fig. 5C,D). By contrast, robust MyHC expression and formation of multinucleated myotubes occurred in MyoD-transfected *PS1*$^{-/-}$ MEFs maintained under identical high-serum conditions (Fig. 5C,D). Under low-serum (2% FBS) conditions, MyoD-transfected *PS1*$^{-/-}$ MEFs also had higher MyHC levels than control-transfected WT MEFs (data not shown). We next investigated whether this MyoD-induced myogenesis in *PS1*$^{-/-}$ MEFs could be 'rescued' by PS1. Transfection with PS1 expression vectors completely inhibited the MyoD-induced myogenic differentiation of *PS1*$^{-/-}$ MEFs (Fig. 7K).

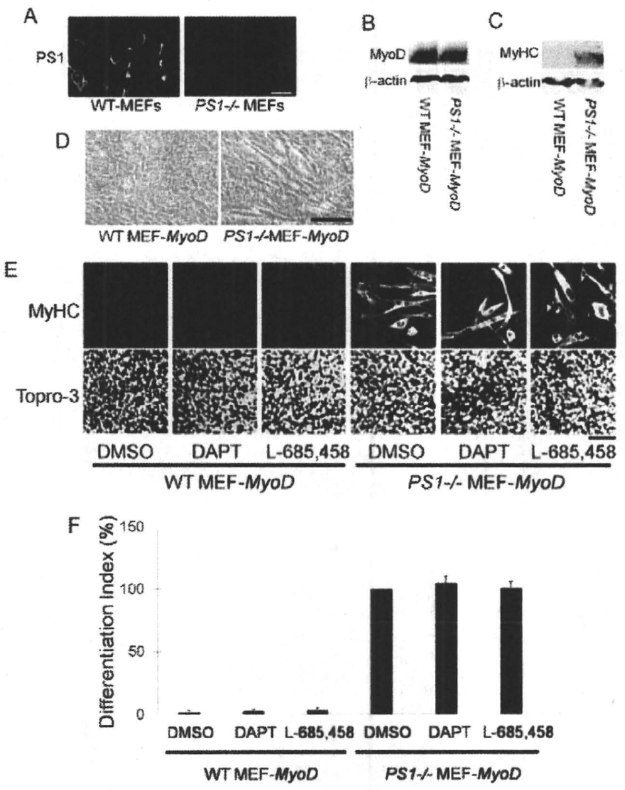

Fig. 5. Induced myogenic differentiation of *PS1*$^{-/-}$ MEFs is independent of γ-secretase activity. *PS1*$^{-/-}$ mice die during embryogenesis and so, to examine myogenesis, we used MyoD-transfected MEFs. (A) Immunostaining revealed that PS1 is expressed by WT MEFs, but is absent from *PS1*$^{-/-}$ MEFs. (B,C) Immunoblot analysis demonstrated that myogenesis was effectively induced in *PS1*$^{-/-}$ MEFs by transfection of a MyoD-expression vector. β-actin was the protein loading control. (C,D) Culture in high-serum (10% FBS) medium for 5 days still resulted in MyHC expression (C) and formation of myotubes (D) in *PS1*$^{-/-}$ MEFs, but not in WT. (E,F) WT MEFs transfected with the MyoD-expression-vector and exposed to 1 μM DAPT or 1 μM L-685,458 to inhibit γ-secretase activity failed to induce MyHC expression when cultured in 10% FBS for 5 days. However, MyoD-transfected *PS1*$^{-/-}$ MEFs, maintained under identical culture conditions, differentiated and expressed MyHC, with inhibition of γ-secretase activity having no effect on the differentiation index. Data from at least three independent experiments are shown ± s.d. Scale bars: 20 μm (A), 100 μm (D) and 60 μm (E).

To determine whether this process is independent of γ-secretase activity, we used the γ-secretase inhibitors DAPT and L-685,458 on MyoD-transfected *PS1*$^{-/-}$ MEFs and WT MEFs. γ-secretase activity was significantly decreased in WT MEFs (~93%) after 1 μM DAPT treatment, as determined using a γ-secretase activity detection kit (data not shown). We found that neither treatment with DAPT (even up to 50 μM; data not shown) nor L-685,458 could induce myogenic differentiation in MyoD-expressing WT MEFs in high-serum medium, or changed high MyHC expression levels in MyoD-containing *PS1*$^{-/-}$ MEFs (Fig. 5E and quantified in 5F). Together, these observations suggest that the MyoD-induced myogenic program is inhibited by PS1 in a manner that is independent of γ-secretase activity.

PS1 regulates Id1 expression in myogenic cells

Despite the high-serum culture conditions, our results show that myogenic differentiation is clearly induced by ectopic MyoD expression in *PS1*$^{-/-}$ MEFs (Fig. 5). BMP (bone morphogenetic protein) signalling contributes to serum-induced inhibition of myogenic differentiation in vitro (Kodaira et al., 2006) and *Id1* is a major BMP signalling downstream target gene, known to be a potent negative regulator of MyoD in myoblasts (Benezra et al., 1990; Jen et al., 1992; Katagiri et al., 2002). We hypothesised therefore, that Id1 might also be regulated by PS1. To test this, immunostaining was performed to investigate whether satellite cells express Id1 during myogenic progression. Id1 was not detectable in Pax7^{+} quiescent satellite cells (T0), but was upregulated in activated and proliferating satellite cells (T72; Fig. 6A). Id1 was then downregulated in myoblasts committing to myogenic differentiation, as shown by the presence of Myog or absence of Pax7 (arrow; Fig. 6A,B), showing that the Id1 expression profile mirrors that of PS1 (Fig. 1).

To determine whether the levels of PS1 and Id1 were causally linked in myoblasts, we transfected satellite-cell-derived myoblasts with *pMSCV-PS1-IRES-GFP* and found high Id1 levels in eGFP^{+} (PS1-expressing) cells (Fig. 6C). Constitutive PS1 expression in C2C12 cells also resulted in upregulation of the level of Id1 protein on immunoblots (Fig. 6D and quantified in 6E). Consistent with the observations that PS1 promotes Id1, knockdown of PS1 levels using siRNA in C2C12 myoblasts, led to a dramatic decrease in Id1 expression levels (Fig. 6F). Constitutive PS1 expression did not influence Pax7 protein levels (Fig. 4I), and in accord with this, increased Id1, did not change Pax7 expression in C2C12 myoblasts transfected with *pCMV-Id1* (Fig. 6G).

PS1 regulates Id1 expression with a γ-secretase independent mechanism

Constitutive PS1 expression still caused an increase in Id1 in C2C12, even when γ-secretase activity was inhibited using DAPT (Fig. 6D,E). This response was not restricted to myogenic cells, however: in the mesenchymal stem cell line 10T1/2, constitutive PS1 expression again increased Id1 protein levels, independently of γ-secretase activity (Fig. 7A). To further examine PS1 regulation of Id1, we performed immunocytochemical analysis to assay Id1 protein in *PS1*$^{-/-}$ MEFs, and found that Id1 expression was lower in *PS1*$^{-/-}$ MEFs than in WT MEFs. This was again independent of γ-secretase activity because inhibition with DAPT did not influence Id1 expression in WT MEFs (Fig. 7B). This decreased level of Id1

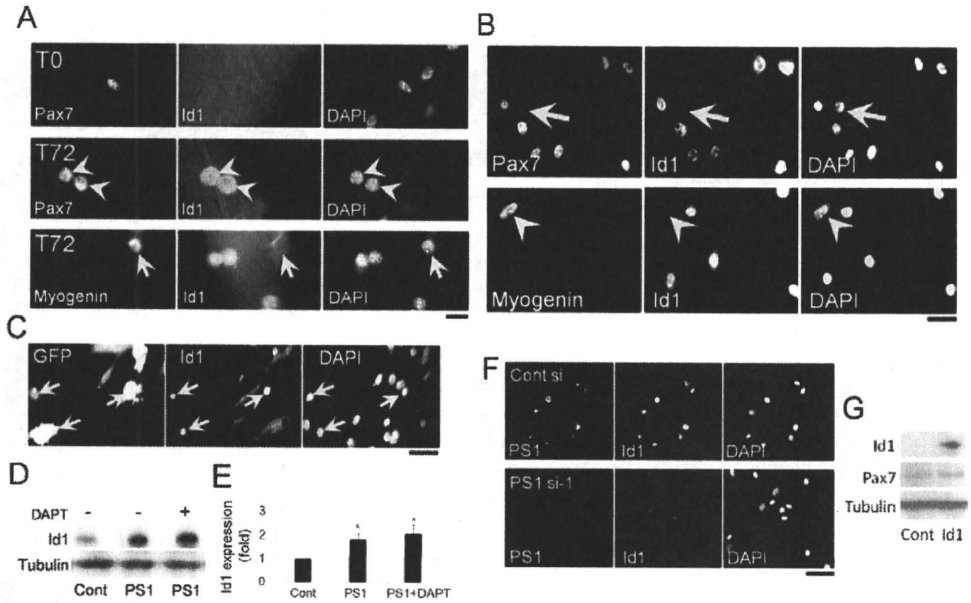

Fig. 6. PS1 regulates the expression of Id1, to function independently of Notch signalling. (A) Immunocytochemical analysis for Pax7 and Id1 on satellite cells associated with a myofibre demonstrated that Id1 was not present in quiescent satellite cells (T0). By 72 hours (T72) after isolation, Id1 was robustly expressed in Pax7-expressing cells (arrowheads), but downregulated in satellite-cell-derived myoblasts as they commit to myogenic differentiation (arrows), as shown by co-immunostaining for Id1 and Myog. (B) In plated satellite-cell-derived myoblasts, again Id1 expression was associated with undifferentiated cells (arrows, $Pax7^-$ cells; arrowheads, $Myog^+$ cells). (C) Constitutive expression of PS1 by transfection of satellite-cell-derived myoblasts with *pMSCV-PS1-IRES-eGFP* resulted in eGFP (PS1)-containing cells also having robust Id1 expression, revealed by immunostaining (arrows, GFP^+Id1^+ cells). (D) Immunoblotting of C2C12 myoblasts transfected with a PS1-expression vector (PSI) showed that Id1 levels were significantly increased. This PS1-induced increase in Id1 levels was not affected by exposure to 1 μM DAPT for 6 hours to inhibit γ-secretase activity (quantified in E). (F) The effect of *PS1* siRNA on expression of Id1 in satellite-cell-derived myoblasts was analysed by immunostaining, and demonstrated that PS1 and Id1 were colocalised in cells transfected with control siRNA (Cont), but revealed that siRNA-mediated knockdown of PS1 resulted in less Id1 expression. (G) Immunoblotting analysis showed that constitutive Id1 expression did not change Pax7 expression levels in C2C12 myoblasts transfected with the *pCMV-Id1* expression vector. Data from at least three independent experiments are shown ± s.d. Asterisks in E indicate that data are significantly different from control values ($P<0.05$). Scale bars: 10 μm (A), 20 μm (B), 30 μm (C) and 50 μm (F).

protein in $PS1^{-/-}$ MEFs was also confirmed by immunoblotting (Fig. 7C). Because MyoD-induced myogenesis in $PS1^{-/-}$ MEFs could be 'rescued' by PS1 (Fig. 7K), we also transfeced $PS1^{-/-}$ MEFs with the Id1 expression vector, *pCMV-Id1*, and again found a complete inhibition of MyoD-induced myogenic differentiation in high-serum medium (Fig. 7K).

To separately confirm that PS1 regulates Id1 in a γ-secretase-activity-independent manner, we used a mutant *PS1* (*D385C PS1*) that encodes a PS1 protein with an Asp385 mutation that completely abolishes γ-secretase activity but still allows complex formation (Tolia et al., 2006). $PS1^{-/-}PS2^{-/-}$ MEFs stably expressing *D385C PS1* and another line carrying a control PS1 (*Cys-less PS1*) with full γ-secretase activity, both produced protein, as shown by immunostaining with PS1 (N-terminal) antibody (Fig. 7D). As expected, *D385C PS1* was not recognised by an anti-PS1 (cleaved loop domain) antibody that detected the *Cys-less PS1* control (Fig. 7E) (Tolia et al., 2006). Crucially, Id1 protein was increased in both $PS1^{-/-}PS2^{-/-}$ MEFs expressing *D385C-PS1* and control $PS1^{-/-}PS2^{-/-}$ MEFs expressing *Cys-less PS1* (Fig. 7E-G), demonstrating again that γ-secretase activity is not required for PS1-mediated Id1 upregulation.

PS1, but not PS2, regulates Id1 expression

There is evidence that PS1 and PS2 might have partially overlapping functions (reviewed by Vetrivel et al., 2006). However, the reduced Id1 levels found in $PS1^{-/-}$ MEFs was not observed in $PS2^{-/-}$ MEFs, whose Id1 levels were comparable with WT MEFs (Fig. 7B). To specifically test the effects of PS2 on Id1 expression, we performed immunoblot analysis in C2C12 myoblasts transfected with *PS2* siRNA and found that the significantly reduced PS2 protein levels did not affect Id1 (Fig. 7H quantified in 7I,J), in contrast to the effects of *PS1* siRNA (Fig. 6F). Furthermore, $PS2^{-/-}$ MEFs are refractory to MyoD-induced myogenic differentiation in high-serum culture conditions, in contrast to $PS1^{-/-}$ MEFs, confirming that there are non-redundant functions between the PS1 and PS2 (Fig. 7K).

PS1 knockdown accelerates myogenic differentiation in regenerating skeletal muscle in vivo

Finally, we evaluated the significance of PS1 to regenerating muscle in vivo. Cardiotoxin was used to induce muscle damage in the gastrocnemius of adult C57BL/6N mice and 12 hours later, the muscle was directly injected with 50 μl of 10 μM siRNA in Atelocollagen, a potent siRNA delivery mediator in vivo (Kinouchi et al., 2008). Four different conditions were used: saline control, control siRNA, PS1 si-1 and PS1 si-2. Regenerating muscles were isolated 3.5 days after cardiotoxin injection and frozen in liquid nitrogen before being cryosectioned. Muscle regeneration was assayed by immunostaining muscle sections for developmental MyHC (dMyHC), which is transiently expressed in regenerating myofibres, and phosphorylated histone H3 (p-histone H3) was used as a proliferation marker (Fig. 8). PS1 knockdown resulted in a significant induction of dMyHC expression (Fig. 8A and quantified

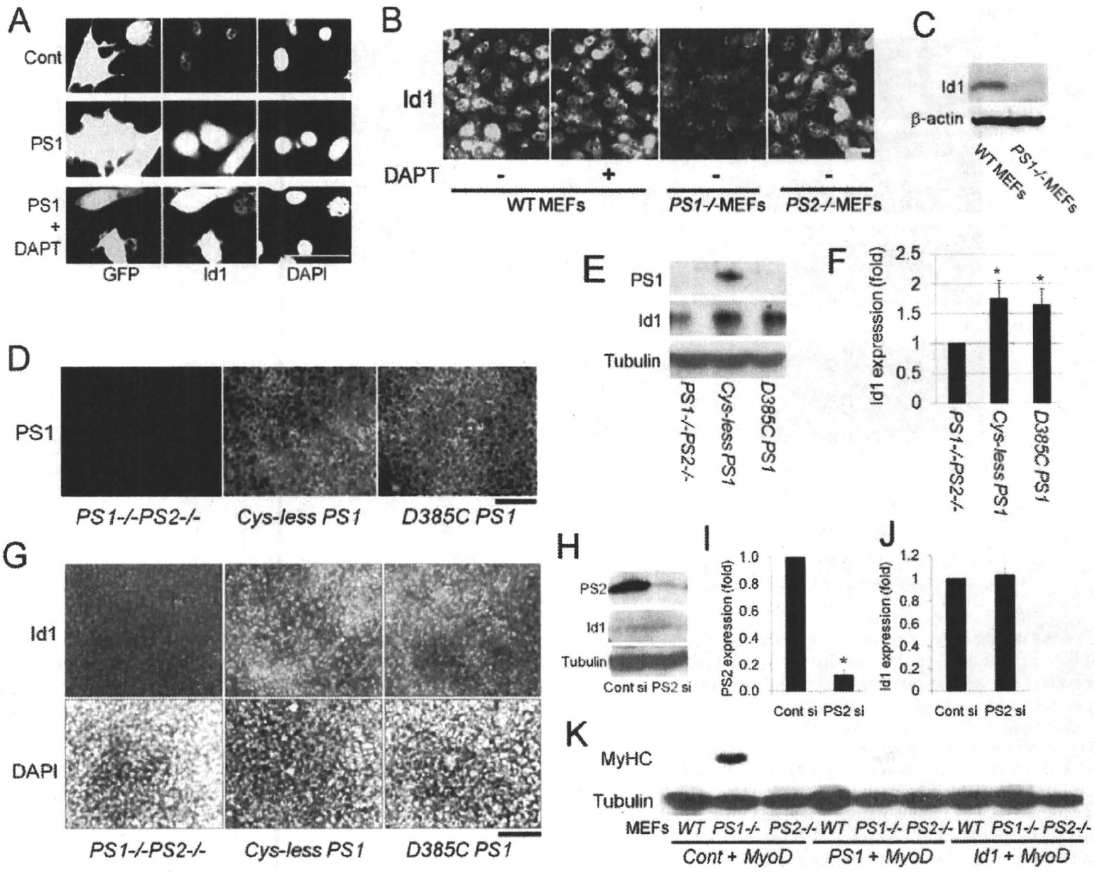

Fig. 7. PS1 controls Id1 expression in non-muscle cells via a γ-secretase-activity-independent mechanism. (A) PS1-regulated Id1 expression was not restricted to myogenic cells: in the mesenchymal stem cell line 10T1/2, immunostaining showed that constitutive PS1 expression increased Id1 protein levels, which was also independent of γ-secretase activity, as shown by exposure to 1 μM DAPT for 6 hours. (B) Immunostaining showed that reduction in Id1 levels was specific to *PS1*$^{-/-}$ MEFs because *PS2*$^{-/-}$ MEFs had robust Id1 levels, comparable to WT MEFs. Exposure of WT MEFs to 1 μM DAPT for 12 hours did not result in a reduction in Id1 levels. (C) Although Id1 was clearly present in WT MEFs, immunoblot analysis demonstrated that Id1 was expressed at very low levels from *PS1*$^{-/-}$ MEFs. β-actin was used as a control for protein loading. (D) Immunostaining showed that anti-PS1 (N-terminal) antibody recognised both stably inserted *D385C PS1* (PS1 mutant with no γ-secretase activity) and control *Cys-less PS1* in *PS1*$^{-/-}$*PS2*$^{-/-}$ MEFs. (E) Immunoblot analysis revealed that PS1 protein in *D385C-PS1*-inserted *PS1*$^{-/-}$*PS2*$^{-/-}$ MEFs was not detected by anti-PS1 (cleaved loop domain) antibody, which recognised the *Cys-less PS1*-inserted *PS1*$^{-/-}$*PS2*$^{-/-}$ MEFs. (E,F). Id1 protein was increased in both *Cys-less PS1* and *D385C-PS1* expressing *PS1*$^{-/-}$*PS2*$^{-/-}$ MEFs (quantified in F). (G) Immunostaining confirmed that *D385C PS1* inserted into *PS1*$^{-/-}$PS2$^{-/-}$ MEFs can upregulate Id1 protein, as does the control *Cys-less PS1*-inserted *PS1*$^{-/-}$*PS2*$^{-/-}$ MEFs. (H) Immunoblot analysis illustrates that specific siRNA-mediated knockdown of PS2 does not affect the level of Id1 protein in C2C12 myoblasts (quantified in I,J). (K) Immunoblotting 5 days after transfection illustrated that the presence of a MyoD-expression vector resulted in myogenic differentiation in *PS1*$^{-/-}$ MEFs maintained in high-serum culture conditions, as shown by the presence of MyHC. By contrast, WT or *PS2*$^{-/-}$ MEFs did not undergo myogenic conversion. Importantly, co-transfection of the MyoD expression vector with either a PS1-expression vector, or an Id1-expression vector, largely blocked this induction of MyHC in *PS1*$^{-/-}$ MEFs. Tubulin was used as an internal control for protein loading. Data from at least three independent experiments are shown ± s.d. Asterisks in F, I and J indicate whether data are significantly different from control values ($P<0.05$). Scale bars: 30 μm (A), 10 μm (B) and 100 μm (D,G).

in 8B) and a significant reduction in the number of cells containing p-histone H3 (Fig. 8C and quantified in 8D) compared with control siRNA. These observations indicate that PS1 is required for maintenance of proliferating cells and inhibition of myogenic differentiation during muscle regeneration in vivo as well as in vitro.

Discussion

Understanding how the decision between self-renewal and differentiation is regulated in satellite cells is central to understanding how skeletal muscle maintains a viable stem cell compartment. Here, we show that the multifunctional protein PS1 is able to direct muscle satellite cells away from myogenic differentiation and towards the self-renewal phenotype. Although PS1 is a key component of the γ-secretase complex, we found that PS1 also acts through γ-secretase-independent mechanisms to affect satellite cell fate, by controlling Id1 protein.

Satellite cells are normally mitotically quiescent in mature muscle, so must first be activated to enter the cell cycle and generate myoblasts (Zammit, 2008). Important pathways associated with activation include sphingolipid (Nagata et al., 2006b; Nagata et al., 2006a), p38MAPK (Jones et al., 2005) and Notch signalling (Conboy and Rando, 2002). Notch signalling in proliferating satellite cells plays a role in expanding the satellite cell pool after activation, while preventing precocious differentiation (Conboy et al., 2003; Conboy and Rando, 2002; Kitzmann et al., 2006; Kopan et al., 1994; Kuang et al., 2007; Nofziger et al., 1999). When PS1

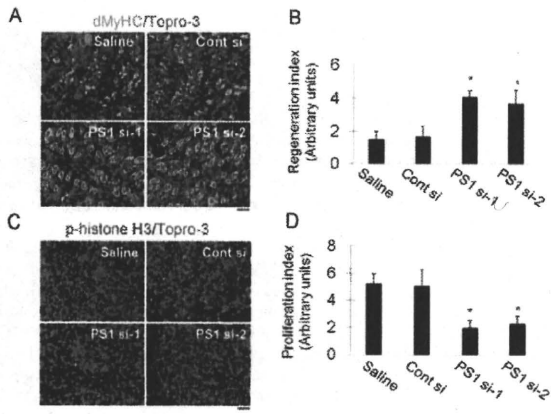

Fig. 8. PS1 maintains proliferation and inhibits precocious differentiation during muscle regeneration in vivo. Regeneration was induced in mouse gastrocnemius muscles by injection of cardiotoxin and, 12 hours later, injection of 50 µl of 10 µM siRNA in Atelocollagen. We employed four different conditions: saline control, control siRNA, PS1si-1 and PS1si-2. Then, 3.5 days after cardiotoxin injection, the muscles were removed, frozen and cryosectioned. (A,B) Muscle regeneration was assayed by immunostaining with Topro-3 for developmental MyHC (dMyHC), which is transiently expressed in regenerating muscle. PS1 knockdown resulted in a significant induction of dMyHC expression compared to controls (quantified in B). (C,D) Immunostaining for phosphorylated histone H3 (p-histone H3) was used as a proliferation marker. A significant reduction of p-histone $H3^+$ cells was observed in muscles exposed to siRNAs against PS1, compared with controls (quantified in D). The bar charts of regeneration index (B) or proliferation index (D) were calculated from the staining intensity of dMyHC-stained regenerating fibres (from A) or the number of p-histone H3-stained proliferating cells (from C), divided by the total number of nuclei in the field of randomly selected sections (n=5 for each condition). Values are means ± s.d. Asterisks in B and D indicate that data are significantly different from values obtained using control siRNA (P<0.05). Scale bars: 70 µm.

is knocked down using siRNA, we observe an increase in cells undergoing myogenic differentiation, with fewer expressing Pax7; a similar phenotype to that observed when Notch signalling is prevented by inhibiting γ-secretase activity using pharmacogical reagents such as DAPT and L-685,458 (Kitzmann et al., 2006; Kuang et al., 2007). Considering the crucial role of PS1 in the γ-secretase complex, PS1 knockdown will directly affect Notch signalling and so some effects on satellite cells are due to perturbation of this pathway. Importantly, not all effects of siRNA knockdown of PS1 in myoblasts could be reproduced by simply inhibiting γ-secretase activity. For example, PS1 knockdown in myoblasts maintained even under high serum conditions, resulted in a high degree of myogenic differentiation, an observation not repeated when only γ-secretase activity was inhibited (Fig. 4B). Therefore, PS1 is also operating independently of its role in the γ-secretase complex. We found that PS1 knockdown also reduces the level of Id1 protein in C2C12 myoblasts. Id1 has been shown to dimerise with basic helix-loop-helix transcription factors such as MyoD, and to inhibit their transcriptional activity (Benezra et al., 1990; Jen et al., 1992). Therefore, reduced Id1 levels would alleviate a block on MyoD transcriptional activity and so lead to induction of Myog and myogenic differentiation. Myog has been shown to indirectly inhibit Pax7 expression (Olguin et al., 2007), thus providing a mechanism by which differentiation and self-renewal are linked through MyoD transcriptional activity. Furthermore, it has been reported that inhibition of myogenic differentiation by forced expression of Notch ICD is not accompanied by *Id1* induction in C2C12 myoblasts (Nofziger et al., 1999), again indicating that this role of PS1 is not operating through Notch signalling.

Several studies have reported that overexpression of PS1 alone is insufficient for enhancing γ-secretase activity, without concomitant overexpression of other members of the complex, including nicastrin, Aph-1 and Pen-2 (reviewed by De Strooper, 2003; Parks and Curtis, 2007; Vetrivel et al., 2006). Therefore, when we used expression vectors to constitutively express only PS1, γ-secretase activity should not have been enhanced. Indeed, myoblasts with constitutive expression of PS1 did not show altered levels of the ICD of either Notch1 or Notch2, or of Hes1 (Fig. 4I). However, to ensure that the effects of PS1 were uncoupled from any caused by increasing γ-secretase activity, we also employed, in parallel, potent inhibitors of γ-secretase activity (DAPT and L-685,458).

Constitutive expression of PS1 resulted in approximately fourfold more transfected satellite-cell-derived myoblasts with Pax7 protein than found in controls, and a significant inhibition of myogenic differentiation. Importantly, inhibiting γ-secretase activity with DAPT did not prevent these effects of constitutive PS1 expression, showing that PS1 acts independently of Notch signalling. Constitutive PS1 expression causes Id1 levels to be increased, presumably allowing more Id1 dimerisation with MyoD and inhibition of myogenic differentiation. Therefore, the failure of MyoD to induce Myog probably prevents the inhibition of Pax7 (Olguin et al., 2007).

We further explored the effects of PS1 on myogenesis using mouse cells with two null alleles of *PS1* (De Strooper et al., 1999; Herreman et al., 2000). *PS1*-null mice die in utero and so we examined MyoD-induced myogenesis in $PS1^{-/-}$ MEFs. Ectopic MyoD was able to efficiently induce myogenesis in $PS1^{-/-}$ MEFs maintained under high-serum conditions, and inhibition of γ-secretase activity with either DAPT or L-685,458 did not prevent this. By contrast, MyoD could not induce myogenesis under similar conditions in WT or $PS2^{-/-}$ MEFs (Fig. 7K), with or without concomitant γ-secretase inhibition. Because WT and $PS2^{-/-}$ MEFs had robust Id1 expression but $PS1^{-/-}$ MEFs did not, and co-transfection of MyoD with either PS1 or Id1 prevented myogenic differentiation of $PS1^{-/-}$ MEFs, these observations indicate that PS1, but not PS2, is able to prevent myogenesis by promoting Id1 function. We also independently confirmed that γ-secretase activity is not required for Id1 upregulation by PS1, by using a PS1 mutant that completely lacks γ-secretase activity (Tolia et al., 2006) yet still increases Id1 levels (Fig. 7).

We have recently shown that β-catenin, probably via canonical Wnt signalling, can influence satellite cell fate, with increased β-catenin levels promoting the self-renewal phenotype (Perez-Ruiz et al., 2008). Interestingly, it has been shown that PS1 can interact with various armadillo family members, including β-catenin (reviewed by Parks and Curtis, 2007; Vetrivel et al., 2006). PS1 binds β-catenin and can regulate β-catenin stability, in both positive and negative ways (Meredith et al., 2002; Vetrivel et al., 2006; Zhang et al., 1998). Specific inhibition of BMP signalling results in myogenic differentiation in high-serum culture conditions (Kodaira et al., 2006), and Id1 is a major effector of BMP signalling (Katagiri et al., 2002). We did not find any differences between WT and $PS1^{-/-}$ MEFs in the expression of proteins known to be upstream of Id1, such as pSmad1/5/8 and Egr-1 (our unpublished observations). Pharmacological blockade has shown that interactions between PS1 and β-catenin are independent of γ-secretase activity (Meredith et

al., 2002) and, as mentioned above, Notch ICD is not accompanied by *Id1* induction in C2C12 myoblasts (Nofziger et al., 1999). Thus, speculatively, PS1 might operate through its effects on β-catenin stability to affect canonical Wnt signalling to control Id1, independently of its γ-secretase activity.

PS1 is also known to regulate Ca^{2+} homeostasis through γ-secretase-independent mechanisms (Akbari et al., 2004; Tu et al., 2006). In regenerating muscles, Id1 can be negatively regulated by Calcineurin, a Ca^{2+}-calmodulin-dependent serine/threonine protein phosphatase (Sakuma et al., 2005), so PS1 might also control Id1 protein through the regulation of Ca^{2+} homeostasis. Id1 protein is also known to be controlled by protein stabilisation (Bounpheng et al., 1999), so PS1 might also more directly control Id1 expression through such a mechanism.

Taken together, our data provide evidence of a novel mechanism operating in stem cells, whereby PS1 controls Id1 to regulate the transcriptional activity of bHLH transcription factors, operating independently of γ-secretase activity. In the neural system for example, PS1 is essential for maintenance of the neural progenitor cell pool and for preventing neural differentiation in the developing brain (Hitoshi et al., 2002). In adults, proliferating neural progenitor cells strongly express PS1, but mature neurones do not (Wen et al., 2002). Importantly, Id1 negatively regulates neurogenic transcription factors such as Mash1 in brain (Nakashima et al., 2001; Vinals et al., 2004), paralleling its actions on MyoD in muscle. Speculatively therefore, PS1 might have a common role in maintaining the progenitor cell pool via regulation of Id1 in both muscle and brain. The demonstration of a PS1-Id1 signalling network might also provide new insight into the pathogenesis of mutated PS1-related early-onset familial Alzheimer's disease (reviewed by Parks and Curtis, 2007; Vetrivel et al., 2006).

In conclusion, our study shows that PS1 acts as a potent regulator of fate choice in muscle satellite cells. Undoubtedly, some of the effects of PS1 on satellite cell function are due to its role as a crucial component of the γ-secretase complex, central to Notch signalling. However, PS1 also operates in a γ-secretase-independent manner to control MyoD, and our results show that this is probably achieved through regulation of Id1. The mechanisms that promote satellite cell self-renewal for the maintenance of the stem cell pool and those that prevent precocious myogenic differentiation must be linked and feedback on each other to carefully regulate the extent of differentiation for repair, versus maintenance, of a viable stem cell pool, able to respond to future needs. PS1 control of MyoD transcriptional activity would appear to be one of these links between differentiation and self-renewal mechanisms.

Materials and Methods

Isolation and culture of primary satellite cells and myoblasts

Adult (8-12 weeks old) C57BL10 mice were killed by cervical dislocation, and the extensor digitorum longus (EDL) muscles isolated and digested in collagenase as previously described (Beauchamp et al., 2000). Myofibres and associated satellite cells were isolated and cultured in plating medium (DMEM supplemented with 10% horse serum, 0.5% chicken embryonic extract, 4 mM L-glutamine and 1% penicillin-streptomycin) at 37°C in 5% CO_2, as described previously (Perez-Ruiz et al., 2008). Satellite cells were removed from myofibres by enzymatic treatment with 0.125% trypsin-EDTA solution for 10 minutes at 37°C and maintained in high-serum-containing medium (DMEM supplemented with 20% FBS, 1% chicken embryo extract, 10 ng/ml FGF, 4 mM L-glutamine and 1% penicillin-streptomycin). This medium supported both proliferation and differentiation of satellite cell progeny when bFGF was removed. The C2 (Yaffe and Saxel, 1977) subclone C2C12 and 10T1/2 cell lines were obtained from Riken Cell Bank (Tsukuba, Japan). C2C12 cells were maintained in growth medium (GM; F-10 medium supplemented with 20% FBS and antibiotics). For myogenic differentiation (both C2 and satellite cells), the culture medium was replaced with differentiation medium (DM; DMEM containing 2% horse serum and antibiotics) for 72 hours at 37°C. 10T1/2 cells, WT, *PS1*$^{-/-}$, *PS2*$^{-/-}$, *PS1*$^{-/-}$*PS2*$^{-/-}$ MEFs and *PS1*$^{-/-}$*PS2*$^{-/-}$ MEFs expressing *Cys-less PS1* or *D385C PS1* (Herreman et al., 1999; Herreman et al., 2003) were maintained in DMEM containing 10% FBS and antibiotics.

Antibodies and Reagents

Antibodies were obtained from the following sources: mouse and rabbit anti-PS1 antibodies from Millipore (Bedford, MA); mouse anti-GFP from Roche (Basel, Switzerland); rabbit anti-PS2 antibody from Abcam; mouse anti-Notch1 antibody from BD Biosciences; rat anti-Ki67 from DAKO; goat anti-PS1 antibody, rabbit anti-Id1 antibody, rabbit anti-Hes1 antibody goat anti-Notch2 antibody and rabbit anti-MyoD antibody were obtained from Santa Cruz (Santa Cruz, CA); mouse anti-developmental myosin heavy chain (dMyHC) antibody from Novocastra (Newcastle, UK); mouse anti-MyHC (MF20), anti-Pax7 antibody, anti-Myog antibody (F5D) and anti-tubulin antibody (E7) were obtained from the DSHB (Iowa City, IA); rabbit anti-p-histone H3 antibody from Cell Signaling Technology (Beverly, MA) and Topro-3, rabbit anti-GFP antibody and mouse anti-V5 antibody from Invitrogen (Carlsbad, CA). Mounting medium containing DAPI was purchased from Vector Laboratories (Burlingame, CA). Nuclei were counterstained with either DAPI or Topro-3. DAPT and L-685,468 were purchased from Peptide Institute (Osaka, Japan) and dissolved and applied in DMSO. γ-secretase activity was measured using a γ-secretase activity detection kit according to the manufacturer's instructions (R&D Systems).

Immunoblot analysis

Immunoblot analysis was performed as previously described (Ono et al., 2006). Rabbit or mouse anti-PS1 (recognise loop domain), anti-PS2, anti-MyHC, anti-tubulin, anti-Pax7, anti-Notch1, anti-Notch2, anti-Hes1, anti-MyoD, anti-Id1 or anti-β-actin antibody were applied at 4°C overnight. Horseradish-peroxidase-conjugated secondary antibodies were used for visualisation by chemiluminescence with a digital luminescent image analyser LAS-1000 (Fujifilm, Tokyo, Japan).

Immunostaining

Immunocytochemistry was performed as previously described (Ono et al., 2007). Primary antibodies were used in PBS as follows: goat anti-PS1 (recognises N-terminal), anti-Id1, anti-Ki67, anti-MyHC, anti-Pax7, anti-Myog, mouse anti-GFP, rabbit anti-GFP, anti-V5 or anti-MyoD antibody at 4°C overnight. For immunohistochemistry, frozen muscle cross-sections were fixed with cold acetone, blocked with M.O.M kit (Vector Laboratories) and incubated with either anti-dMyHC or p-histone H3 antibody. Immunostained myofibres and plated cells were viewed on a Zeiss Axiophot 200M using Plan-Neofluar lenses, or on a Nikon C1si confocal using Plan-Fluor lenses. Digital images were acquired with a Zeiss AxioCam HRm Charge-Coupled Device using AxioVision software version 4.4. Images were optimised globally and assembled into figures using Adobe Photoshop.

RNA interference in vitro

The transfection of siRNA (Stealth siRNA; Invitrogen) into C2C12 myoblasts and primary muscle progenitors cells was performed using Lipofectamine 2000 reagent (Invitrogen) as previously described (Ono et al., 2007). Transfection of siRNA into single myofibres was carried out 20-24 hours after isolation. All samples were examined 72 hours after the transfection. The following siRNA sequences were used: *PS1* siRNA-1, 5′-ACTCTCTTTCCAGCTCTTATCTATT-3′; *PS1* siRNA-2, 5′-GCACCTTTGTCCTACTTCCAGAATG-3′; and *PS2* siRNA, 5′-CCACUAUCAA-GUCUGUGCGUUUCUA-3′. The control siRNA sequence and AlexaFlour488-conjugated siRNA were purchased from Invitrogen.

Plasmid construction and transfection

PS1 cDNA was cloned into *pMSCV-IRES-GFP* (Zammit et al., 2006) or *pCMV-V5*-expression vectors to generate *pMSCV-PS1-IRES-GFP* or *pCMV-PS1-V5* respectively. Transfection was performed once or twice (10 hours after the first transfection) using Lipofectamine 2000 (Invitrogen) or Lipofectamine LTX (Invitrogen) with Plus Reagents (Invitrogen) in accordance with the manufacturer's instructions.

Muscle injury and in vivo siRNA transfection

Male 8-week old C57BL/6N mice were used according to the Guidelines and Regulations for Laboratory Animal Care of Tohoku University Graduate School of Medicine. Muscle damage was induced by direct intramuscular injection of 50 μl of 10 μM cardiotoxin (Sigma) into the belly of gastrocnemius muscle using a 29G 1/2 insulin syringe. For in vivo siRNA transfection, siRNA duplexes were incubated with Atelocollagen (Koken, Japan) according to the manufacturer's instructions.

Statistical analysis

Data are presented as mean ± standard deviation. Comparisons among groups were determined by the Student's *t*-test. *P* values of <0.05 were considered to be statistically significant.

We would like to thank: Bart De Strooper (Center for Human Genetics, Katholieke Universiteit Leuven) for kindly providing the *Cys-less PS1* and *D385C PS1* constructs, and WT, *PS1*$^{-/-}$, *PS2*$^{-/-}$,

PS1$^{-/-}$*PS2*$^{-/-}$ MEFs and *PS1*$^{-/-}$*PS2*$^{-/-}$ MEFs expressing *Cys-less PS1* or *D385C PS1*; Douglas Melton and Robert Benezra for generously sharing constructs *pCMV-MyoD* and *pcDNA3-mId1*, respectively through Addgene; the Pax7, Myog, tubulin and MF20 antibodies, developed by A. Kawakami, W. E. Wright, M. Klymkowsky and D. A. Fischman, respectively, were obtained from the Developmental Studies Hybridoma Bank developed under the auspices of the NICHD and maintained by the University of Iowa; and Frederico Calhabeu and Paul Knopp for much help. Y.O. received support from Tohoku University research fellowships and is now funded by the Muscular Dystrophy Campaign (grant number RA3/737). V.F.G. is supported by the Medical Research Council (grant number G0700307). This work was supported in part by a research grant from the Uehara Memorial Foundation. The laboratory of P.S.Z. is also supported by the Association of International Cancer Research and the Wellcome Trust. Deposited in PMC for release after 6 months.

References

Akbari, Y., Hitt, B. D., Murphy, M. P., Dagher, N. N., Tseng, B. P., Green, K. N., Golde, T. E. and LaFerla, F. M. (2004). Presenilin regulates capacitative calcium entry dependently and independently of gamma-secretase activity. *Biochem. Biophys. Res. Commun.* **322**, 1145-1152.

Beauchamp, J. R., Heslop, L., Yu, D. S., Tajbakhsh, S., Kelly, R. G., Wernig, A., Buckingham, M. E., Partridge, T. A. and Zammit, P. S. (2000). Expression of CD34 and Myf5 defines the majority of quiescent adult skeletal muscle satellite cells. *J. Cell Biol.* **151**, 1221-1234.

Benezra, R., Davis, R. L., Lockshon, D., Turner, D. L. and Weintraub, H. (1990). The protein Id: a negative regulator of helix-loop-helix DNA binding proteins. *Cell* **61**, 49-59.

Bounpheng, M. A., Dimas, J. J., Dodds, S. G. and Christy, B. A. (1999). Degradation of Id proteins by the ubiquitin-proteasome pathway. *FASEB J.* **13**, 2257-2264.

Brack, A. S., Conboy, I. M., Conboy, M. J., Shen, J. and Rando, T. A. (2008). A temporal switch from notch to Wnt signaling in muscle stem cells is necessary for normal adult myogenesis. *Cell Stem Cell* **2**, 50-59.

Collins, C. A., Olsen, I., Zammit, P. S., Heslop, L., Petrie, A., Partridge, T. A. and Morgan, J. E. (2005). Stem cell function, self-renewal, and behavioral heterogeneity of cells from the adult muscle satellite cell niche. *Cell* **122**, 289-301.

Conboy, I. M. and Rando, T. A. (2002). The regulation of Notch signaling controls satellite cell activation and cell fate determination in postnatal myogenesis. *Dev. Cell* **3**, 397-409.

Conboy, I. M., Conboy, M. J., Smythe, G. M. and Rando, T. A. (2003). Notch-mediated restoration of regenerative potential to aged muscle. *Science* **302**, 1575-1577.

De Strooper, B. (2003). Aph-1, Pen-2, and Nicastrin with Presenilin generate an active gamma-Secretase complex. *Neuron* **38**, 9-12.

De Strooper, B., Annaert, W., Cupers, P., Saftig, P., Craessaerts, K., Mumm, J. S., Schroeter, E. H., Schrijvers, V., Wolfe, M. S., Ray, W. J. et al. (1999). A presenilin-1-dependent gamma-secretase-like protease mediates release of Notch intracellular domain. *Nature* **398**, 518-522.

Esselens, C., Oorschot, V., Baert, V., Raemaekers, T., Spittaels, K., Serneels, L., Zheng, H., Saftig, P., De Strooper, B., Klumperman, J. et al. (2004). Presenilin 1 mediates the turnover of telencephalin in hippocampal neurons via an autophagic degradative pathway. *J. Cell Biol.* **166**, 1041-1054.

Halevy, O., Piestun, Y., Allouh, M. Z., Rosser, B. W., Rinkevich, Y., Reshef, R., Rozenboim, I., Wleklinski-Lee, M. and Yablonka-Reuveni, Z. (2004). Pattern of Pax7 expression during myogenesis in the posthatch chicken establishes a model for satellite cell differentiation and renewal. *Dev Dyn.* **231**, 489-502.

Hansson, E. M., Lendahl, U. and Chapman, G. (2004). Notch signaling in development and disease. *Semin. Cancer Biol.* **14**, 320-328.

Herreman, A., Hartmann, D., Annaert, W., Saftig, P., Craessaerts, K., Serneels, L., Umans, L., Schrijvers, V., Checler, F., Vanderstichele, H. et al. (1999). Presenilin 2 deficiency causes a mild pulmonary phenotype and no changes in amyloid precursor protein processing but enhances the embryonic lethal phenotype of presenilin 1 deficiency. *Proc. Natl. Acad. Sci. USA* **21**, 11872-11877.

Herreman, A., Serneels, L., Annaert, W., Collen, D., Schoonjans, L. and De Strooper, B. (2000). Total inactivation of gamma-secretase activity in presenilin-deficient embryonic stem cells. *Nat. Cell Biol.* **2**, 461-462.

Herreman, A., Van Gassen, G., Bentahir, M., Nyabi, O., Craessaerts, K., Mueller, U., Annaert, W. and De Strooper, B. (2003). gamma-Secretase activity requires the presenilin-dependent trafficking of nicastrin through the Golgi apparatus but not its complex glycosylation. *J. Cell Sci.* **116**, 1127-1136.

Hitoshi, S., Alexson, T., Tropepe, V., Donoviel, D., Elia, A. J., Nye, J. S., Conlon, R. A., Mak, T. W., Bernstein, A. and van der Kooy, D. (2002). Notch pathway molecules are essential for the maintenance, but not the generation, of mammalian neural stem cells. *Genes Dev.* **16**, 846-858.

Huppert, S. S., Ilagan, M. X., De Strooper, B. and Kopan, R. (2005). Analysis of Notch function in presomitic mesoderm suggests a gamma-secretase-independent role for presenilins in somite differentiation. *Dev. Cell* **8**, 677-688.

Jarriault, S., Brou, C., Logeat, F., Schroeter, E. H., Kopan, R. and Israel, A. (1995). Signalling downstream of activated mammalian Notch. *Nature* **377**, 355-358.

Jen, Y., Weintraub, H. and Benezra, R. (1992). Overexpression of Id protein inhibits the muscle differentiation program: in vivo association of Id with E2A proteins. *Genes Dev.* **6**, 1466-1479.

Jones, N. C., Tyner, K. J., Nibarger, L., Stanley, H. M., Cornelison, D. D., Fedorov, Y. V. and Olwin, B. B. (2005). The p38alpha/beta MAPK functions as a molecular switch to activate the quiescent satellite cell. *J. Cell Biol.* **169**, 105-116.

Katagiri, T., Imada, M., Yanai, T., Suda, T., Takahashi, N. and Kamijo, R. (2002). Identification of a BMP-responsive element in Id1, the gene for inhibition of myogenesis. *Genes Cells* **7**, 949-960.

Kinouchi, N., Ohsawa, Y., Ishimaru, N., Ohuchi, H., Sunada, Y., Hayashi, Y., Tanimoto, Y., Moriyama, K. and Noji, S. (2008). Atelocollagen-mediated local and systemic applications of myostatin-targeting siRNA increase skeletal muscle mass. *Gene Ther.* **15**, 1126-1130.

Kitzmann, M., Bonnieu, A., Duret, C., Vernus, B., Barro, M., Laoudj-Chenivesse, D., Verdi, J. M. and Carnac, G. (2006). Inhibition of Notch signaling induces myotube hypertrophy by recruiting a subpopulation of reserve cells. *J. Cell Physiol.* **208**, 538-548.

Kodaira, K., Imada, M., Goto, M., Tomoyasu, A., Fukuda, T., Kamijo, R., Suda, T., Higashio, K. and Katagiri, T. (2006). Purification and identification of a BMP-like factor from bovine serum. *Biochem. Biophys. Res. Commun.* **345**, 1224-1231.

Kopan, R., Nye, J. S. and Weintraub, H. (1994). The intracellular domain of mouse Notch: a constitutively activated repressor of myogenesis directed at the basic helix-loop-helix region of MyoD. *Development* **120**, 2385-2396.

Kuang, S., Kuroda, K., Le Grand, F. and Rudnicki, M. A. (2007). Asymmetric self-renewal and commitment of satellite stem cells in muscle. *Cell* **129**, 999-1010.

Lammich, S., Okochi, M., Takeda, M., Kaether, C., Capell, A., Zimmer, A. K., Edbauer, D., Walter, J., Steiner, H. and Haass, C. (2002). Presenilin-dependent intramembrane proteolysis of CD44 leads to the liberation of its intracellular domain and the secretion of an Abeta-like peptide. *J. Biol. Chem.* **277**, 44754-44759.

Lepper, C., Conway, S. J. and Fan, C. M. (2009). Adult satellite cells and embryonic muscle progenitors have distinct genetic requirements. *Nature* **460**, 627-631.

Mauro, A. (1961). Satellite cell of skeletal muscle fibers. *J. Biophys. Biochem. Cytol.* **9**, 493-495.

McKinnell, I. W., Ishibashi, J., Le Grand, F., Punch, V. G., Addicks, G. C., Greenblatt, J. F., Dilworth, F. J. and Rudnicki, M. A. (2008). Pax7 activates myogenic genes by recruitment of a histone methyltransferase complex. *Nat. Cell Biol.* **10**, 77-84.

Meredith, J. E., Jr., Wang, Q., Mitchell, T. J., Olson, R. E., Zaczek, R., Stern, A. M. and Seiffert, D. (2002). Gamma-secretase activity is not involved in presenilin-mediated regulation of beta-catenin. *Biochem. Biophys. Res. Commun.* **299**, 744-750.

Nagata, Y., Kobayashi, H., Umeda, M., Ohta, N., Kawashima, S., Zammit, P. S. and Matsuda, R. (2006a). Sphingomyelin levels in the plasma membrane correlate with the activation state of muscle satellite cells. *J. Histochem. Cytochem.* **54**, 375-384.

Nagata, Y., Partridge, T. A., Matsuda, R. and Zammit, P. S. (2006b). Entry of muscle satellite cells into the cell cycle requires sphingolipid signaling. *J. Cell Biol.* **174**, 245-253.

Nakashima, K., Takizawa, T., Ochiai, W., Yanagisawa, M., Hisatsune, T., Nakafuku, M., Miyazono, K., Kishimoto, T., Kageyama, R. and Taga, T. (2001). BMP2-mediated alteration in the developmental pathway of fetal mouse brain cells from neurogenesis to astrocytogenesis. *Proc. Natl. Acad. Sci. USA* **98**, 5868-5873.

Nofziger, D., Miyamoto, A., Lyons, K. M. and Weinmaster, G. (1999). Notch signaling imposes two distinct blocks in the differentiation of C2C12 myoblasts. *Development* **126**, 1689-1702.

Olguin, H. C., Yang, Z., Tapscott, S. J. and Olwin, B. B. (2007). Reciprocal inhibition between Pax7 and muscle regulatory factors modulates myogenic cell fate determination. *J. Cell Biol.* **177**, 769-779.

Ono, Y., Sensui, H., Sakamoto, Y. and Nagatomi, R. (2006). Knockdown of hypoxia-inducible factor-1alpha by siRNA inhibits C2C12 myoblast differentiation. *J. Cell Biochem.* **98**, 642-649.

Ono, Y., Sensui, H., Okutsu, S. and Nagatomi, R. (2007). Notch2 negatively regulates myofibroblastic differentiation of myoblasts. *J. Cell Physiol.* **210**, 358-369.

Parks, A. L. and Curtis, D. (2007). Presenilin diversifies its portfolio. *Trends Genet.* **23**, 140-150.

Perez-Ruiz, A., Ono, Y., Gnocchi, V. F. and Zammit, P. S. (2008). beta-Catenin promotes self-renewal of skeletal-muscle satellite cells. *J. Cell Sci.* **121**, 1373-1382.

Repetto, E., Yoon, I. S., Zheng, H. and Kang, D. E. (2007). Presenilin 1 regulates epidermal growth factor receptor turnover and signaling in the endosomal-lysosomal pathway. *J. Biol. Chem.* **282**, 31504-31516.

Sakuma, K., Nakao, R., Aoi, W., Inashima, S., Fujikawa, T., Hirata, M., Sano, M. and Yasuhara, M. (2005). Cyclosporin A treatment upregulates Id1 and Smad3 expression and delays skeletal muscle regeneration. *Acta Neuropathol.* **110**, 269-280.

Seale, P., Sabourin, L. A., Girgis-Gabardo, A., Mansouri, A., Gruss, P. and Rudnicki, M. A. (2000). Pax7 is required for the specification of myogenic satellite cells. *Cell* **102**, 777-786.

Shen, J., Bronson, R. T., Chen, D. F., Xia, W., Selkoe, D. J. and Tonegawa, S. (1997). Skeletal and CNS defects in Presenilin-1-deficient mice. *Cell* **89**, 629-639.

Skapek, S. X., Rhee, J., Kim, P. S., Novitch, B. G. and Lassar, A. B. (1996). Cyclin-mediated inhibition of muscle gene expression via a mechanism that is independent of pRB hyperphosphorylation. *Mol. Cell. Biol.* **16**, 7043-7053.

Struhl, G. and Greenwald, I. (1999). Presenilin is required for activity and nuclear access of Notch in Drosophila. *Nature* **398**, 522-525.

Tolia, A., Chavez-Gutierrez, L. and De Strooper, B. (2006). Contribution of presenilin transmembrane domains 6 and 7 to a water-containing cavity in the gamma-secretase complex. *J. Biol. Chem.* **281**, 27633-27642.

Tu, H., Nelson, O., Bezprozvanny, A., Wang, Z., Lee, S. F., Hao, Y. H., Serneels, L., De Strooper, B., Yu, G. and Bezprozvanny, I. (2006). Presenilins form ER Ca2+ leak channels, a function disrupted by familial Alzheimer's disease-linked mutations. *Cell* **126**, 981-993.

Vetrivel, K. S., Zhang, Y. W., Xu, H. and Thinakaran, G. (2006). Pathological and physiological functions of presenilins. *Mol Neurodegener.* **1**, 4.

Vinals, F., Reiriz, J., Ambrosio, S., Bartrons, R., Rosa, J. L. and Ventura, F. (2004). BMP-2 decreases Mash1 stability by increasing Id1 expression. *EMBO J.* **23**, 3527-3537.

Wen, P. H., Friedrich, V. L., Jr., Shioi, J., Robakis, N. K. and Elder, G. A. (2002). Presenilin-1 is expressed in neural progenitor cells in the hippocampus of adult mice. *Neurosci. Lett.* **318**, 53-56.

Wilson, C. A., Murphy, D. D., Giasson, B. I., Zhang, B., Trojanowski, J. Q. and Lee, V. M. (2004). Degradative organelles containing mislocalized alpha-and beta-synuclein proliferate in presenilin-1 null neurons. *J. Cell Biol.* **165**, 335-346.

Wong, P. C., Zheng, H., Chen, H., Becher, M. W., Sirinathsinghji, D. J., Trumbauer, M. E., Chen, H. Y., Price, D. L., Van der Ploeg, L. H. and Sisodia, S. S. (1997). Presenilin 1 is required for Notch1 and DII1 expression in the paraxial mesoderm. *Nature* **387**, 288-292.

Yaffe, D. and Saxel, O. (1977). Serial passaging and differentiation of myogenic cells isolated from dystrophic mouse muscle. *Nature* **270**, 725-727.

Yoshida, N., Yoshida, S., Koishi, K., Masuda, K. and Nabeshima, Y. (1998). Cell heterogeneity upon myogenic differentiation: down-regulation of MyoD and Myf-5 generates 'reserve cells'. *J. Cell Sci.* **111**, 769-779.

Zammit, P. S. (2008). All muscle satellite cells are equal, but are some more equal than others? *J. Cell Sci.* **121**, 2975-2982.

Zammit, P. S., Golding, J. P., Nagata, Y., Hudon, V., Partridge, T. A. and Beauchamp, J. R. (2004). Muscle satellite cells adopt divergent fates: a mechanism for self-renewal? *J. Cell Biol.* **166**, 347-357.

Zammit, P. S., Relaix, F., Nagata, Y., Ruiz, A. P., Collins, C. A., Partridge, T. A. and Beauchamp, J. R. (2006). Pax7 and myogenic progression in skeletal muscle satellite cells. *J. Cell Sci.* **119**, 1824-1832.

Zhang, Z., Hartmann, H., Do, V. M., Abramowski, D., Sturchler-Pierrat, C., Staufenbiel, M., Sommer, B., van de Wetering, M., Clevers, H., Saftig, P. et al. (1998). Destabilization of beta-catenin by mutations in presenilin-1 potentiates neuronal apoptosis. *Nature* **395**, 698-702.

Zhang, Z., Nadeau, P., Song, W., Donoviel, D., Yuan, M., Bernstein, A. and Yankner, B. A. (2000). Presenilins are required for gamma-secretase cleavage of beta-APP and transmembrane cleavage of Notch-1. *Nat. Cell Biol.* **2**, 463-465.

Brain, Behavior, and Immunity 23 (2009) 108–115

Contents lists available at ScienceDirect

Brain, Behavior, and Immunity

journal homepage: www.elsevier.com/locate/ybrbi

Acute stress-induced colonic tissue HSP70 expression requires commensal bacterial components and intrinsic glucocorticoid

Kaori Matsuo [a], Xiumin Zhang [b], Yusuke Ono [c], Ryoichi Nagatomi [a,*]

[a] Department of Medicine and Science in Sports and Exercise, Tohoku University Graduate School of Medicine, 2-1 Seiryo-machi, Aoba-ku, Sendai, Japan
[b] School of Public Health, Jilin University, China
[c] Randall Division of Cell and Molecular Biophysics, King's College London, London, UK

ARTICLE INFO

Article history:
Received 1 May 2008
Received in revised form 22 July 2008
Accepted 29 July 2008
Available online 11 September 2008

Keywords:
HSP70
ZO-1
Acute restraint stress
Commensal bacteria
TLR4

ABSTRACT

Induction of heat shock protein (HSPs) has a protective effect in cells under stress. Physical stressors, such as restraint, induce HSPs in colonic tissue *in vivo*, but the mechanism of HSP induction is not yet clear. Because commensal bacteria support basal expression of colon epithelial HSP70, we postulated that stress responses may enhance the interaction of commensal bacteria and the colonic tissue. Restraining C57BL/6 mice for 2 h effectively induced HSP70 in colonic epithelia. Both blockade of stress-induced glucocorticoid by RU486 or elimination of commensal bacteria by antibiotics independently abrogated restraint-induced HSP70 augmentation. Oral administration of LPS to commensal-depleted mice restored restraint-induced HSP70 augmentation. Because TLR4 expression was absent from the epithelial surface, and was limited to lamina propria and muscularis externa, we examined how LPS reaches the lamina propria. Alexa-LPS administered in the colonic lumen was only detected in the lamina propria of the restrained mice. Expression of the tight junction component ZO-1 in the epithelia, which regulates the passage of luminal substances through the epithelia, was reduced after restraint, but reversed by RU486.

In conclusion, HSP70 induction in colonic epithelial cells under restraint requires both stress-induced glucocorticoid and luminal commensal bacteria, and LPS plays a significant role. Glucocorticoid-dependent attenuation of epithelial tight junction integrity may facilitate the access of LPS into the lamina propria, where TLR4, known to be required for HSP70 induction, is abundantly expressed. Sophisticated regulation of colonic protection against stressors involving the general stress response and the luminal environment has been demonstrated.

1. Introduction

Stress episodes are important risk factors for the development and reactivation of intestinal inflammation in rodents (Qiu et al., 1999) and in humans (Levenstein et al., 2000; Stam et al., 1997). Both environmental and psychological stress are known to alter the clinical course of inflammatory bowel disease (IBD) (Danese et al., 2004; Kugathasan et al., 2007; Mawdsley and Rampton, 2005; Tanaka et al., 2007; Tlaskalova-Hogenova et al., 2004). General stress reactions, such as activation of the HPA axis upon acute stress, are commonly accepted as having protective effects (Ader et al., 1979; Besedovsky and Sorkin, 1977; Riley, 1981). However, it has not been well documented how such adaptational reactions occur or are disrupted in the colon.

One of the cellular protective measures against stressors is the induction of HSP expression. HSPs are highly conserved proteins found in all prokaryotes and eukaryotes (Tobian et al., 2004). HSPs serve as molecular chaperones and play a significant role in the protection of cells against various cellular stressors, such as heat (Cvoro et al., 1998; Evdonin et al., 2006; Tomasovic et al., 1983), hypoxia (Dwyer et al., 1989; Zimmerman et al., 1991), ultraviolet irradiation (Kwon et al., 2002; Trautinger et al., 1996), oxidative stress (Drummond and Steinhardt, 1987), or endoplasmic reticulum stress (Yoneda et al., 2004). Unless intracellular HSPs are induced to protect cells exposed to acute stressors, they may undergo apoptosis or necrosis (Yun et al., 1997).

HSPs are also induced in various tissues and organs in response to various psychophysiological stressors (Fleshner et al., 2004; Fukudo et al., 1997), such as restraint (Campisi et al., 2003), ischemia (Kukreja et al., 1994; Lee et al., 2006; Oksala et al., 2002), exercise (Fehrenbach et al., 2005), infection (Ramaglia et al., 2004), inflammation (Ludwig et al., 1999), and hyperthermia (Hotchkiss et al., 1993). Among the various HSPs, HSP70[1] has recently been shown

* Corresponding author. Fax: +81 22 7178589.
E-mail address: nagatomi@m.tains.tohoku.ac.jp (R. Nagatomi).

0889-1591/$ - see front matter © 2008 Elsevier Inc. All rights reserved.
doi:10.1016/j.bbi.2008.07.013

[1] *Abbreviations used:* HSP70, heat shock protein 70; ZO-1,zonula occludens-1; TLR4, Toll-like receptor 4; RU486, mifepristone; LPS, lipopolysaccharide; ELISA, enzyme-linked immunosorbent assay.

to exhibit a protective role in gut epithelial cells (Liu et al., 2003). However, the mechanism by which such protective HSP70 is induced in the colon has not been determined.

We assumed roles of activation of the HPA axis and sympathetic nervous system in colon HSP70 expression as well as the contribution of commensal bacteria in stress-induced HSP70 expression, as basal HSP70 expression in gut epithelial cells has been reported to be dependent on commensal bacteria through interactions with TLR4 (Rakoff-Nahoum et al., 2004).

Interestingly, TLR4, which is responsive for bacterial lipopolysaccharides in the intestinal tissue, was shown to be located mainly at the lamina propria and absent at the epithelial surface (Rumio et al., 2006). TLR4 in the colonic tissue would also exhibit a similar distribution. For luminal bacterial components to interact with TLR4, we postulated that tight junction integrity of the gut epithelia may be altered under stress facilitating access of luminal bacterial components to the lamina propria TLR4 and finally inducing HSP70.

In the present study, therefore, we first examined colonic HSP70 under acute stress, and then examined the involvements of luminal bacteria and stress-induced corticosterone in HSP70 induction in colonic epithelia. In addition, we examined the expression of the tight junction component ZO-1 in the colonic tissue before and after stress.

2. Methods

2.1. Animals

Male C57BL/6 mice and green fluorescence protein (GFP) transgenic mice (C57BL/6 background) were purchased from the mouse supply centre of Tohoku University School of Medicine, and used for the experiments at 10–12 weeks of age. Five or six mice were housed together per cage (30 × 25 × 17.5 cm) and were given free access to food and water. Animals were maintained under specific pathogen-free conditions on a daily 12-h light/dark cycle. Drinking bottles, cages, sawdust, and rodent chow for mice were all autoclaved before use as described previously (Kanemi et al., 2005). Mice were housed in freshly sterilized cages with fresh sawdust every day. All experiments were performed in accordance with the Guidelines and Regulations for Laboratory Animal Care of Tohoku University Medical School.

2.2. Restraint stress procedure

The stressor used in this study was restraint (Fukui et al., 1997; Kanemi et al., 2005; Sudo et al., 1997). Each experimental male C57BL/6 or GFP mouse was placed for 2 h in 50-ml centrifuge tubes. The walls of the tubes were stripped in part to avoid an acute rise in the body temperature. The restraint experiment was carried out in the morning between 8:00 and 10:00. Non-restraint mice of the same age were kept in their home cage throughout the restraint procedure. Animals were given no access to food or water during restraint stress treatment. Immediately after restraint stress, restrained and non-restrained mice were sacrificed by anesthesia.

2.3. In vivo RU486 and propranolol treatment

The glucocorticoid receptor antagonist RU486 was administrated orally (30 mg/kg) in aqueous solution containing 0.25% carboxymethylcellulose and 0.2% polysorbate 80 (Sigma, St. Louis, MO, USA) in a volume of 5 ml/kg through a gastric feeding tube (Concordet and Ferry, 1993; Zhang et al., 2005a,b).

RU486 or an equivalent volume of vehicle (0.25% carboxymethylcellulose and 0.2% polysorbate 80) was given 30 min before the 2-h restraint session.

2.4. Depletion of colonic commensal bacteria

Depletion of colonic commensal bacteria was performed according to the method reported by Rakoff-Nahoum et al. (2004) with minor modifications by daily administration of 0.2 ml of the following antibiotic cocktail *via* a ball-tipped gastric feeding tube for 7 days and by supplementing the drinking water with a 2-fold dilution of antibiotic cocktail during the same 7-day period. The antibody cocktail contained ampicillin (1 mg/ml), vancomycin (0.5 mg/ml), neomycin sulfate (1 mg/ml), and metronidazole (1 mg/ml) (all from Sigma).

2.5. Lipopolysaccharide (LPS) administration to antibiotic-treated mice

Following antibiotic treatment, mice were given a daily supplement of 0.2 ml distilled water containing 50 μg/ml of purified *Escherichia coli* 026:B6 LPS (Sigma) through a gastric feeding tube for 5 days. Drinking water during this period was supplemented with LPS (25 μg/ml). A lower dose of LPS did not induce stable augmentation of colonic HSP70. Mice in the control group received the same volume of distilled water according to the same protocol.

2.6. Anesthesia

Sevoflurane (Abbott Japan, Tokyo, Japan) inhalation was used to anesthetize the animals. A volume of less than 2 ml of anesthetic was evaporated into a container of approximately 500 ml at room temperature. The mice were then placed into the container and anesthetized within 15 s (Kanemi et al., 2005).

2.7. Blood sampling, catecholamines, and corticosterone assay

Blood samples were collected from the axillary artery of anesthetized mice and transferred immediately into either heparinized or untreated stock tubes for plasma and serum sampling, respectively. After blood sampling, animals were euthanized by deep anesthesia with sevoflurane.

Blood samples were centrifuged at 3000 rpm for 10 min at 4 °C to obtain plasma or serum. Plasma and serum samples were stored at −80 °C until assay. Catecholamines were quantified by column-switching high-performance liquid chromatography (HPLC) with fluorometric detection (Dutton et al., 1999; Nohta et al., 1987). Serum corticosterone level was measured using a rat corticosterone-H^3 RIA kit (ICN Biomedicals, Costa Mesa, CA, USA), in accordance with the manufacturer's instructions.

2.8. Rectal temperature

The rectal temperature of the mice was measured with a digital thermometer (CTM-303 model; Terumo, Kanagawa, Japan) at a distance of 2.5 mm from the anus. Measurements were obtained at ambient room temperature (20–23 °C). The rectal temperatures of control and stressed mice were measured at 30-min intervals, for a total of 120 min ($n = 5$).

2.9. Bacterial culture

For determination of colonic microflora, fecal matter was removed from the colon using sterile technique. The contents were diluted and plated on universal and differential media for the growth of anaerobes and aerobes under anaerobic or aerobic culture conditions. AnaeroPack (Mitsubishi Gas Chemical Company, Niigata, Japan) was used to detect anaerobic flora. The numbers of colonies per mg of feces (wet weight) were counted after incubation at 37 °C for 48 h (aerobes) and 72 h (anaerobes).

2.10. Colonic tissue preparation

The mid-portion, approximately 1 cm, of total colon—transverse colon—was excised immediately after the restraint session and stored at −80 °C until examination. After determining the frozen weight of colon samples, colonic tissue was lysed with lysis buffer consisting of 40 mM Tris (pH 7.5), 300 mM KCl, 1% Triton X-100, 2 mM EDTA, with protease inhibitor cocktail (1:20) (Sigma). Colonic tissue was dissected using scissors and further homogenized using a Polytron Aggregate homogenizer (Kinematica, Luzern, Switzerland). The extracts were cleared by centrifugation at 21,000*g* for 10 min. Aliquots of prepared samples were kept frozen at −80 °C until ELISA or Western blotting analysis.

2.11. ELISA for HSP70

HSP70 concentration in the extract was quantified by enzyme-linked immunosorbent assay (ELISA) using a commercially available HSP70 kit (StressXpress HSP70 ELISA; Stressgen Biotechnologies, Victoria, BC, Canada) in accordance with the manufacturer's instructions.

2.12. Western blotting analysis

Equal amounts of protein from the supernatant of colonic tissue samples quantified by the Lowry method were electrophoresed on 12% SDS–polyacrylamide gels and transferred electrophoretically onto polyvinylidene difluoride membranes (Millipore, Bedford, MA, USA). After blocking with 5% non-fat milk in phosphate buffered saline (PBS) containing 0.1% Tween 20 for 1 h at room temperature, membranes were incubated with rabbit polyclonal anti-HSP70 antibody (1:1000) (Stressgen), rabbit polyclonal anti-TLR4 (H-80) antibody (1:500) (Santa Cruz Biotechnology, CA, USA), rat polyclonal anti-ZO-1 antibody (1:250) (Santa Cruz), and mouse monoclonal anti-β-actin antibody (1:2000) (Sigma) in TBS (pH 8.0) containing 0.05% Tween 20 (TBST) at 4 °C overnight and washed three times for 5 min with PBS. The membranes were then incubated with either HRP-conjugated secondary anti-rat IgG (1:1000) or anti-mouse IgG (1:1000) (Cell Signaling Technology, MA, USA) antibody in TBST for 1 h at room temperature, washed three times for 5 min with PBS, and visualized by chemiluminescence using an ECL immunoblotting kit (Cell Signaling) with a digital luminescent image analyzer (LAS-1000; Fujifilm, Tokyo, Japan).

2.13. Immunohistochemistry

The colon samples from male C57BL/6 mice were rapidly embedded in Tissue-Tek OCT compound (Sakura Finetechnical, Tokyo, Japan), frozen in isopentane, pre-cooled in liquid nitrogen, and finally transferred into liquid nitrogen. The tissue blocks were stored at −80 °C prior to cutting. Colonic tissues on slides were fixed in PBS containing 4% paraformaldehyde at room temperature for 20 min, blocked, and penetrated in blocking solution (Dako, Kyoto, Japan) containing 0.3% Triton X-100 for 30 min at room temperature, and incubated overnight with rabbit polyclonal anti-HSP70 antibody (1:500, Stressgen), goat polyclonal anti-TLR4 (L-14) antibody (1:200) (Santa Cruz), and rat polyclonal anti-ZO-1 (R40.76) antibody (1:50) (Santa Cruz) in TBS (pH 8.0) containing 0.01% Triton X-100 at 4 °C overnight. Washes were performed with PBS. The sections were incubated with the secondary antibodies, Alexa Fluor 555-conjugated donkey anti-rabbit IgG (1:400) (Invitrogen, Carlsbad, CA), Alexa Fluor 488-conjugated donkey anti-goat IgG (1:400) (Invitrogen), and Alexa Fluor 488-conjugated goat anti-rat IgG (1:400) (Invitrogen) with nuclear stain marker Topro-3 in TBS (pH 8.0) containing 0.01% Triton X-100 for 1 h at room temperature. The reaction was examined by confocal microscopy (Nikon, Tokyo, Japan).

2.14. Ligated colon loop assays and processing of colonic tissues

Mouse ligated colon loop assays were performed as described previously by Mantis et al. with some modifications (Mantis et al., 2002). During the procedure, mice were maintained under sevoflurane anesthesia. Alexa-LPS 548 was injected into ligated colon loops (1 cm) at a concentration of 1/10 μl. After 10 min, mice were sacrificed by cervical dislocation and the colon was excised immediately. Portions of tested loops were taken and fixed in Tissue-Tek OCT compound (Sakura Finetechnical), frozen in isopentane, pre-cooled in liquid nitrogen, and finally transferred into liquid nitrogen. Colon sections of the specimens were prepared using standard procedures for immunohistochemical analyses.

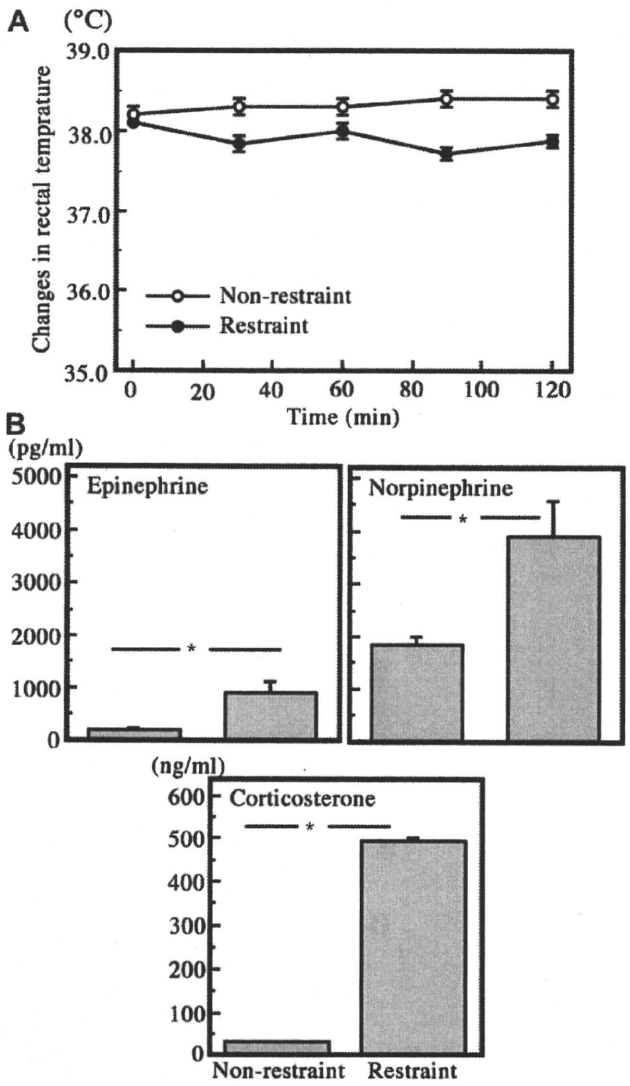

Fig. 1. Restraint did not raise the rectal temperature, but the levels of plasma catecholamine and serum corticosterone were markedly increased. (A) The mean rectal temperature of mice decreased during restraint stress. The results are shown as means ± SE of 5 mice ($^{*}P < 0.05$). (B) Plasma levels of epinephrine and norepinephrine was significantly elevated immediately after restraint stress. Results are shown as means ± SE of 6 mice ($^{*}P < 0.001$). Serum level of corticosterone was significantly elevated immediately after restraint stress. The results are shown as means ± SE of 5 mice ($^{*}P < 0.001$).

2.15. Statistical analysis

Results are presented as the means ± SE. We examined the statistical significance of differences using the two-way analysis of variance (ANOVA). *Post hoc* analysis was carried out using Scheffe's test. Statistical significance was defined as follows: $^{*}P < 0.05$, $^{**}P < 0.01$, $^{***}P < 0.001$.

3. Results

3.1. Restraint stress did not raise the rectal temperature of mice

First, we examined whether there was a rise in rectal temperature in response to restraint stress, because a rise in the rectal temperature may involve HSP70 induction in the colonic tissue (Fig. 1A). The mean rectal temperature of mice decreased gradually during restraint stress, while there was virtually no change in the rectal temperature of non-restrained mice ($n = 5$, $P < 0.05$).

3.2. Restraint stress-induced elevation of plasma catecholamine and corticosterone levels

The plasma levels of epinephrine and norepinephrine were significantly elevated immediately after restraint stress ($P < 0.05$, Student's *t*-test) (Fig. 1B).

The serum level of corticosterone was significantly elevated immediately after restraint stress ($P < 0.001$, Student's *t*-test) (Fig. 1B).

The plasma levels of epinephrine and norepinephrine of antibiotics treated mice were significantly elevated immediately after restraint stress (non-restraint: epinephrine 260.0 ± 50.7 pg/ml, norepinephrine 1806.0 ± 593.9 pg/ml *vs.* restraint: epinephrine 1157.5 ± 193.2 pg/ml, norepinephrine 4438.8 ± 184.0 pg/ml, $n = 4$; $P < 0.05$, Student's *t*-test).

The serum level of corticosterone of antibiotics treated mice was significantly elevated immediately after restraint stress (non-restraint: 36.8 ± 12.7 ng/ml, restraint: 501.1 ± 28.5 ng/ml, $n = 4$; $P < 0.001$, Student's *t*-test).

Thus, antibiotics treatment did not affect the neurohumoral stress response to restraint.

3.3. Restraint stress enhances colonic HSP70

The effects of 2-h restraint on colonic HSP70 were examined both by ELISA (Fig. 2A) and by immunohistochemical analysis (Fig. 2B). HSP70 level in the colonic extract was significantly elevated immediately after restraint as compared to the non-restraint group ($P < 0.001$) (Fig. 2A). Immunohistochemical analyses indicated a detectable basal level of HSP70 expression, but that it was dominantly expressed at the apical or luminal cytoplasm of colonic epithelia. HSP70 expression was weaker in the cells in deeper crypts as compared to those closer to the tips (Fig. 2B). This expression pattern was unchanged after restraint stress, but the degree of HSP70 expression was enhanced after restraint.

3.4. Glucocorticoid receptor antagonist suppressed restraint-induced colonic HSP70 augmentation

Blockade of glucocorticoid by oral administration of RU486 before restraint completely abolished the augmentation of colonic HSP70 and even resulted in down-regulation to below the level of expression in non-restrained mice (basal level) (Fig. 2C). There were no significant differences in HSP70 level between non-restrained and restrained mice treated with RU486 (NS, Fig. 2C). Immunohistochemical analysis revealed no apparent morphological differences between RU486-treated and untreated colon tissue notwithstanding restraint (Fig. 2D). Colonic HSP70 augmentation after restraint was absent in RU486-treated mice.

3.5. Depletion of commensal bacteria abrogates restraint-induced colonic HSP70 augmentation

As commensal bacteria contribute to HSP expression in the gut tissue (Rakoff-Nahoum et al., 2004), the involvement of commensal bacteria in stress-induced HSP70 augmentation was examined.

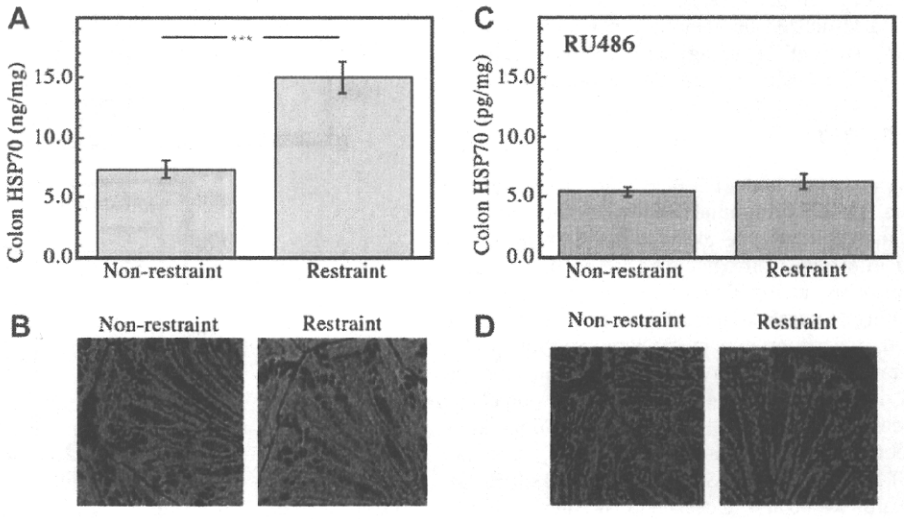

Fig. 2. Colonic HSP70 expression was markedly augmented after 2-h restraint. The augmentation of HSP70 expression was abrogated by RU486 administration. (A) The level of colonic HSP70 was significantly elevated immediately after restraint as compared with non-restrained controls. The results are shown as means ± SE of 8 mice ($^{***}P < 0.001$). (B) Immunohistochemical analysis indicated concentrated expression of colonic HSP70. HSP70: red; Topro-3: blue (200×). (C) No significant difference was found in the HSP70 level between non-restrained and restrained mice treated with RU486. The results are shown as means ± SE of 8 mice. (D) Immunohistochemical analysis revealed no apparent morphological differences in the levels of colonic HSP70 between non-restrained and restrained mice treated with RU486. No HSP70 augmentation after restraint was observed in RU486-treated mice. HSP70: red; Topro-3: blue (200×). There was a significant group × time interaction in repeated-measures ANOVA analysis ($p = 0.0005$, $F = 15.4$).

There were no differences between the changes in body weight of water- and antibiotic-treated mice (water *vs.* antibiotics NS) (Fig. 3A).

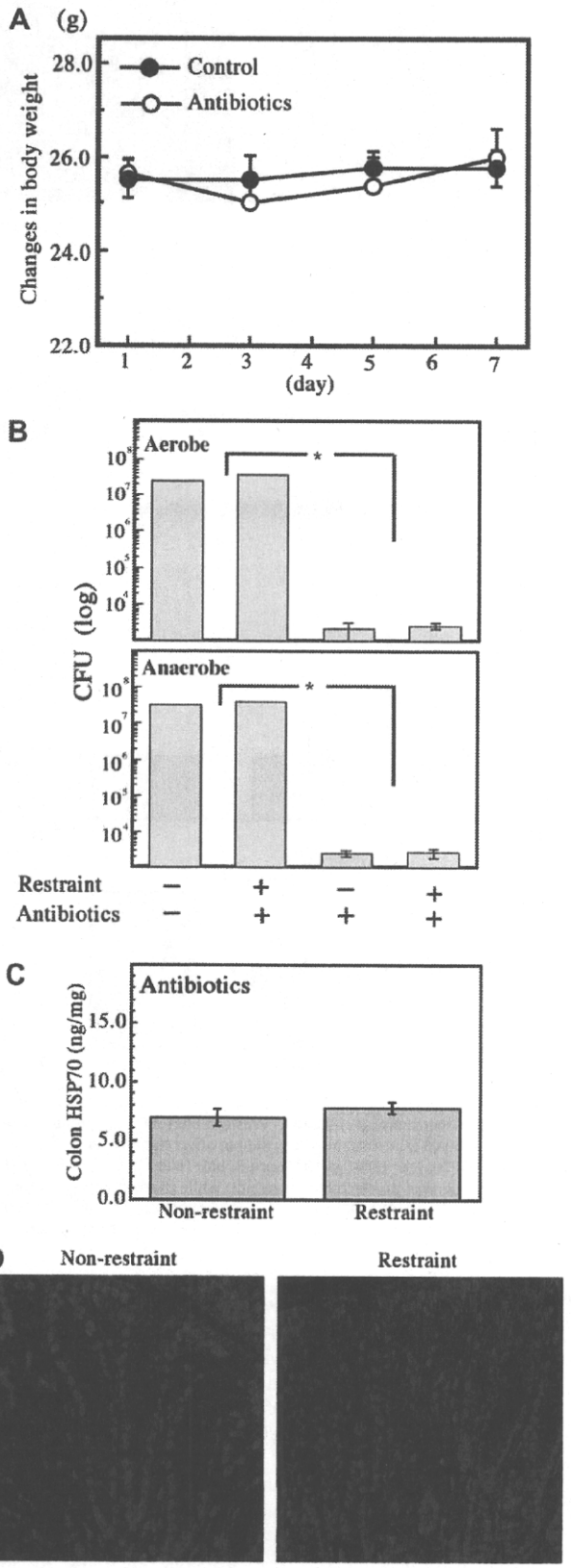

Both anaerobic and aerobic bacteria in the feces sufficiently dropped to less than 1/10,000 of the levels in untreated mice by antibiotic treatment ($n = 8$, $P < 0.001$, Fig. 3B). Restraint did not affect the number of colonies of either aerobic or anaerobic commensal bacteria.

Elimination of commensals abolished restraint-induced HSP70 augmentation (Fig. 3C, 3D). The level of colonic HSP70 of antibiotic-treated restrained mice was 7.75 ± 0.47 ng/ml ($n = 8$), while that in the non-restraint group was 6.93 ± 0.71 ng/ml ($n = 8$) (Fig. 3C). There was no significant difference in the level of HSP70 between the non-restrained and restrained mice. There were no apparent morphological changes, such as damage to the colonic epithelia after antibiotic treatment. Immunohistochemical analyses indicated no apparent enhancement of colonic HSP70 of restrained mice (Fig. 3D).

3.6. *LPS administration partially restores restraint stress-induced colonic HSP70 augmentation of commensal bacteria-depleted mice*

As it has been reported that TLR signaling is required for commensal bacteria-dependent HSP expression (Rakoff-Nahoum et al., 2004), LPS, the ligand for TLR4, was administered to antibiotic-treated mice.

LPS administration alone without restraint did not alter the level of HSP70 ($n = 8$), whereas LPS treatment significantly increased the level of colonic HSP70 in restrained mice ($n = 8$, Fig. 4).

Colonic HSP70 level of mice that received distilled water without LPS did not increase even after restraint stress. Immunohistochemical analyses revealed moderate enhancement of HSP70 in colonic epithelial cells, without apparent morphological changes.

3.7. *TLR4 expression in the colonic tissue was unaffected by restraint stress*

As TLR4 is known to be responsible for LPS-dependent expression of HSP70, the effect of restraint stress on the level of TLR4 expression was examined (Fig. 5).

Immunohistochemical analysis showed that the restraint session had no effect on the level or distribution of TLR4 (Fig. 5A). TLR4 was strongly positive in the muscularis externa as well as in the lamina propria. The level of TLR4 in the colonic tissue was not increased but was slightly down-regulated by restraint stress (Fig. 5B and C).

3.8. *Passage of Alexa-LPS through the colon epithelia by restraint stress*

Next, we examined whether LPS is translocated through the colonic epithelia into the lamina propria after restraint. Immediately after restraint, Alexa-LPS was injected into the looped colonic

Fig. 3. A cocktail of antibiotics was administered for 7 days to eliminate commensal bacteria. Up-regulation of colonic HSP70 expression by restraint was abrogated in antibiotic-treated mice. (A) Effects of antibiotic treatment on body weight changes in C57BL/6 mice. Antibiotic treatment did not affect body weight. The results are shown as means ± SE of 8 mice. (B) Effects of antibiotic treatment on colonic bacterial number (top: aerobe; bottom: anaerobe). Both the colony forming unit (CFU) of anaerobic and aerobic bacteria in the feces dropped to less than 1/10,000 of those from mice without antibiotic treatment. Restraint did not affect the number of colonies of either aerobic or anaerobic commensal bacteria. The results are shown as means ± SE of 8 mice ($^{*}P < 0.001$). (C) There was no significant difference in HSP70 level between non-restrained and restrained mice treated with antibiotics. The results are shown as means ± SE of 8 mice. (D) Immunohistochemical analysis revealed no apparent morphological differences in the levels of colonic HSP70 between non-restrained and restrained mice treated with antibiotics. HSP70 augmentation after restraint was absent in antibiotic-treated mice. HSP70: red; Topro-3: blue (200×).

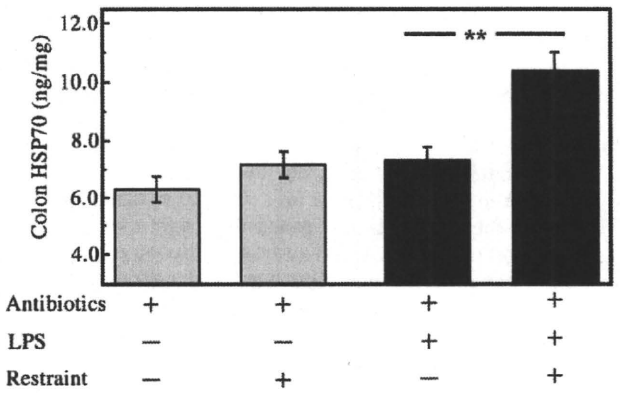

Fig. 4. LPS administration partially restores restraint-induced colonic HSP70 augmentation of commensal bacteria-depleted mice. LPS administration alone without restraint did not alter the level of HSP70, while LPS increased colonic HSP70 level of commensal-depleted restrained mice. Colonic HSP70 level of non-restrained mice, which received distilled water without LPS, did not change even after restraint stress. The results are shown as means ± SE of 8 mice ($^{*}P < 0.01$). There was a significant group × time interaction in repeated-measures ANOVA analysis ($p = 0.0404$, $F = 4.621$).

lumen. After 10 min of incubation, we examined the localization of Alexa-LPS (Fig. 6). Alexa-LPS staining was localized along the luminal surface on the apical membrane of epithelial cells in both control and restrained mice. Interestingly, however, Alexa-LPS staining was rarely detected in the lamina propria of non-restrained mice, but was detectable in the lamina propria of the restrained mice. This result clearly indicated that Alexa-LPS passed through the epithelial barrier of the colon and translocated into the lamina propria after restraint stress.

3.9. Tight junction component ZO-1 was down-regulated after restraint stress

As TLR4 was not expressed on the luminal surface of epithelial cells, we hypothesized that the integrity of tight junctions may be reduced under restraint for LPS or bacterial components to reach TLR4 in the lamina propria. As the level of ZO-1, a component of tight junctions, has been reported to correspond to permeability across a sheet of cultured epithelial cells (Boivin et al., 2007), we examined whether the level of colonic epithelium ZO-1 protein expression was affected by restraint stress (Fig. 7).

Immunohistochemical analysis indicated that ZO-1 staining was localized along the apical membrane of epithelial cells. Restraint resulted in a marked reduction of ZO-1 staining (Fig. 7A).

Western blotting analysis clearly demonstrated that ZO-1 protein level was down-regulated by restraint, in clear contrast to the up-regulation of HSP70 (Fig. 7B and C). The glucocorticoid receptor antagonist RU486 blocked restraint-induced down-regulation of ZO-1 as well as the augmentation of HSP70. ZO-1 level seemed to be enhanced under restraint when RU486 was administered.

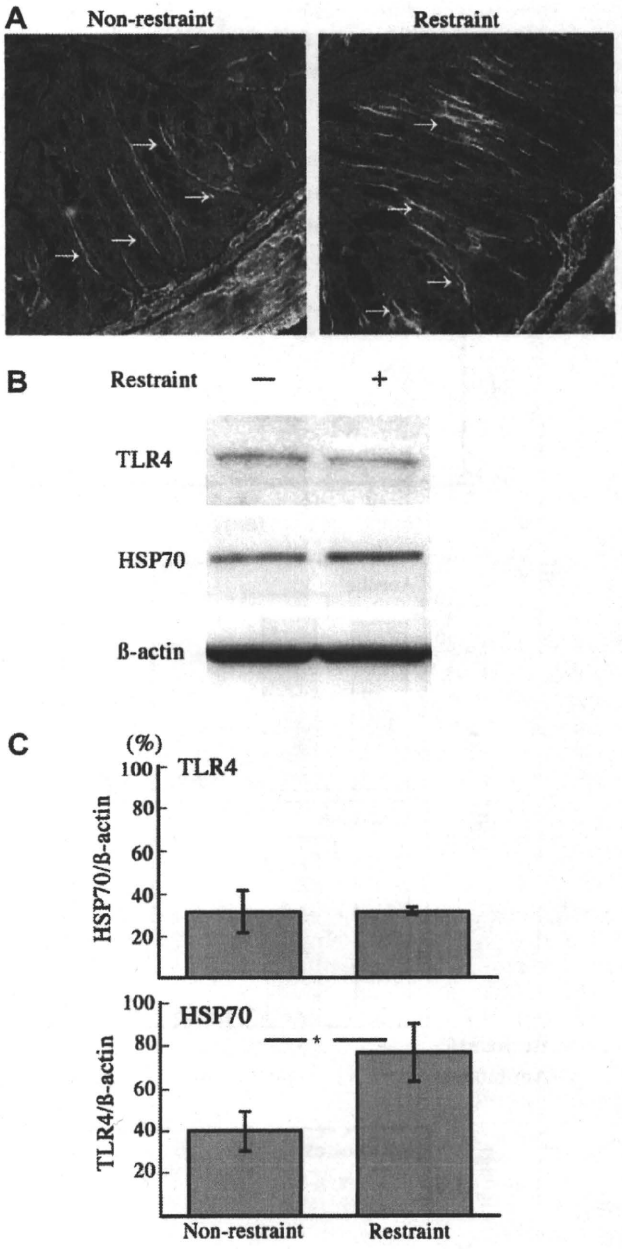

Fig. 5. Effects of 2-h restraint stress on TLR4 and HSP70 expression in colonic tissue (A, immunohistochemistry; B and C, Western blotting). (A) Immunohistochemical analysis showed that restraint stress did not affect the level or distribution of TLR4 (arrow). HSP70: red; TLR4: green; Topro-3: blue (400×). (B) The level of TLR4 in the colonic tissue was unaffected by restraint, while marked augmentation of HSP70 was observed after restraint ($n = 3$). (C) TLR4 expression of the colonic tissue was evaluated by Western blotting analysis in three separate experiments. Standard error of means (SE) is shown as bars.

4. Discussion

To understand how the colon tissue deals with physical stress, we investigated induction of HSP70 by physical stressors in colonic tissue *in vivo*. While baseline HSP70 expression in gut epithelial cells has been reported to be dependent on commensal bacteria (Arvans et al., 2005), we hypothesized that stress-inducible HSP70 expression was dependent on generalized stress reactions due to activation of the HPA axis and/or sympathetic activation.

Restraint-induced HSP70 augmentation was abrogated almost completely by prior administration of RU486, suggesting an essential role of the HPA axis in colonic HSP70 augmentation. Fukudo et al. (1997) reported that water-immersion induced HSP70 in the gut tissue as well as in the brain of rats. Similarly, Udelsman et al.(1994) showed increases in HSP70 in the aorta after restraint stress as well as after dexamethasone administration. They also showed that RU486 effectively reduced the induction of HSP70 in the aortic tissue (Udelsman et al., 1994). Therefore, the glucocorticoid dependence of HSP70 induction may be common in various tissues, including the colon.

Elimination of commensal bacteria by antibiotic treatment did not abrogate baseline HSP70 expression, but markedly abolished

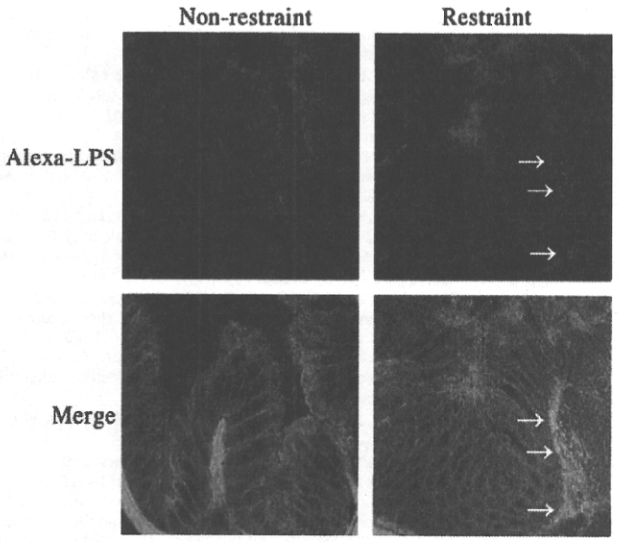

Fig. 6. LPS was translocated to the lamina propria after restraint stress. Immunohistochemical analysis showed that Alexa-LPS (arrow) passed through the mouse colon epithelium with restraint stress. GFP colon tissue: green; Alexa-LPS: red (200×).

stress-induced HSP70 augmentation. As antibiotic treatment alone did not affect the baseline level of corticosterone or the elevation after restraint, our results suggest that stress-induced augmentation of colonic HSP70 requires both glucocorticoid augmentation and colonic microflora.

The requirement for commensal bacteria in restraint stress-induced HSP70 augmentation may be partially replaced by administration of LPS in commensal-depleted mice. As TLR4 is a specific receptor for LPS (Akira and Takeda, 2004), and Rakoff-Nahoum et al. (2004) showed that TLR4 signaling is required for colonic HSP70, the induction of HSP70 by restraint stress observed in this study was likely to be mediated by TLR4.

Interestingly, immunohistochemical examination revealed prominent expression of TLR4 in the lamina propria but not on the epithelial surface. Furrie et al. (2005) reported that TLR4 was only detected in the crypt epithelial cells and was lost as the cells matured and moved toward the gut lumen. Rumio et al. (2006) reported that functional TLR4 is not expressed in the epithelial layer, but its expression is much stronger in the smooth muscle cells and myenteric plexus of human and mouse intestines. They suggested that the low or absent expression of TLR4 on enterocytes may explain the intestinal epithelium hyporesponsiveness to the abundance of LPS in the intestinal lumen.

Then, we examined how luminal bacterial LPS could reach TLR4 in the lamina propria or the muscularis externa. For bacterial LPS to activate TLR4 signaling required for HSP70 induction (Rakoff-Nahoum et al., 2004), LPS must reach the lamina propria or beyond. Although the present study provided no direct evidence that LPS binds to TLR4 at the lamina propria, restraint stress markedly facilitated translocation of LPS to the lamina propria.

Tight junctions at the zonula occludens between epithelial cells form a strong barrier to macromolecules, and the expression and the localization of the tight junction proteins occludin and ZO-1 are known to be directly associated with the membrane permeability of cultured intestinal cells (Dokladny et al., 2006). Down-regulation of ZO-1 protein in the colonic epithelium by restraint stress in this study was glucocorticoid-dependent, as RU486 treatment effectively reversed the down-regulation of colonic epithelial ZO-1 expression. Therefore, we suggest that stress-induced glucocorticoid elevation down-regulated tight junction integrity of the

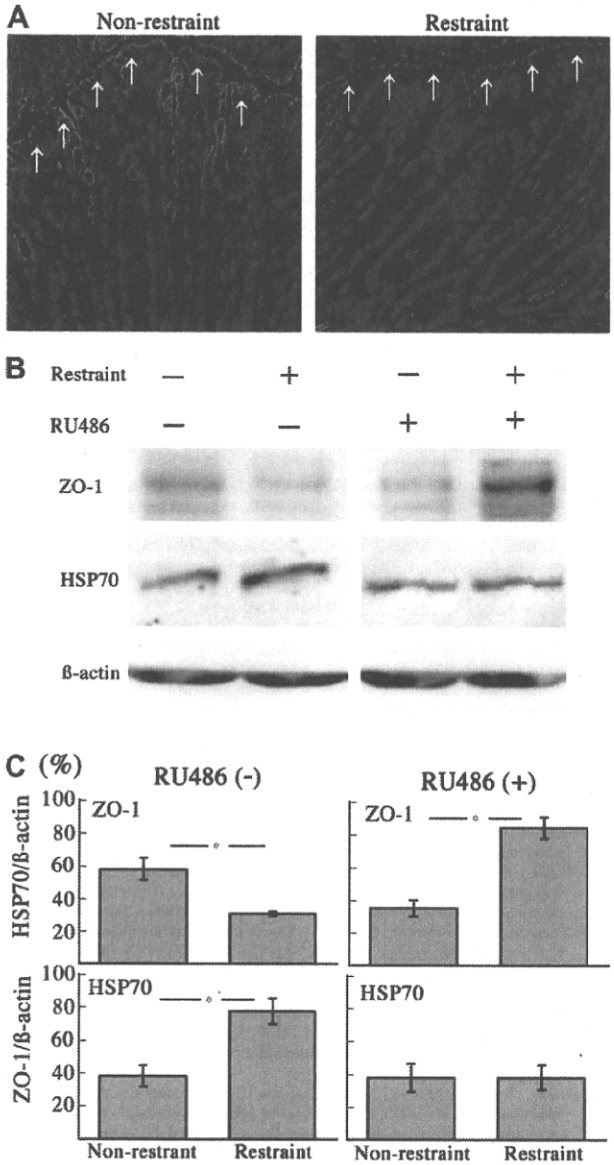

Fig. 7. Tight junction component ZO-1 was down-regulated after restraint. (A, immunohistochemistry; B and C, Western blotting). (A) Immunohistochemical analysis demonstrated that ZO-1 staining (arrow) was localized along the apical portion of the epithelia. Restraint resulted in marked reduction of ZO-1 staining ($n = 3$). ZO-1: green; Topro-3: blue (400×). (B) Western blotting analysis clearly demonstrated that ZO-1 protein level was down-regulated by restraint in clear contrast with the up-regulation of HSP70. The glucocorticoid receptor antagonist RU486 blocked restraint-induced down-regulation of ZO-1. ZO-1 level was rather enhanced under restraint when RU486 was administered ($n = 3$). (C) ZO-1 expression of the colonic tissue was evaluated by Western blotting analysis in three separate experiments. Standard error of means (SE) is shown as bars.

colonic epithelium, resulting in increased translocation of LPS into the lamina propria. Although we lack direct evidence, LPS translocated into the lamina propria may interact with TLR4, resulting in HSP70 expression in the colonic epithelium.

In conclusion, we demonstrated that colonic HSP70 augmentation under physical stress is dependent on endogenous glucocorticoid elevation and luminal bacterial components. We demonstrated that endogenous glucocorticoid elevation reduced tight junction integrity in the colonic epithelium, which facilitated entry of luminal LPS into the lamina propria, where LPS could interact with TLR4 leading to epithelial HSP expression. Although

we still do not know the mechanism by which TLR4 activation in lamina propria led to epithelial HSP70 expression, the results of the present study demonstrated an elaborate and cooperative strategy of stress coping in the colon.

Acknowledgments

We thank Professor Hiroshi Nagura (Division of Athletics and Nutrition, Sendai College, Japan), Dr. Keiko Ishii (Department of Behavioral Neurology and Cognitive Neuroscience, Tohoku University Graduate School of Medicine) for their valuable advice regarding experimental techniques.

References

Ader, R., Cohen, N., Grota, L.J., 1979. Adrenal involvement in conditioned immunosuppression. Int. J. Immunopharmacol. 1, 141–145.
Akira, S., Takeda, K., 2004. Toll-like receptor signalling. Nat. Rev. Immunol. 4, 499–511.
Arvans, D.L., Vavricka, S.R., Ren, H., Musch, M.W., Kang, L., Rocha, F.G., Lucioni, A., Turner, J.R., Alverdy, J., Chang, E.B., 2005. Luminal bacterial flora determines physiological expression of intestinal epithelial cytoprotective heat shock proteins 25 and 72. Am. J. Physiol. Gastrointest. Liver Physiol. 288, G696–G704.
Besedovsky, H., Sorkin, E., 1977. Network of immune–neuroendocrine interactions. Clin. Exp. Immunol. 27, 1–12.
Boivin, M.A., Ye, D., Kennedy, J.C., Al-Sadi, R., Shepela, C., Ma, T.Y., 2007. Mechanism of glucocorticoid regulation of the intestinal tight junction barrier. Am. J. Physiol. Gastrointest. Liver Physiol. 292, G590–G598.
Campisi, J., Leem, T.H., Fleshner, M., 2003. Stress-induced extracellular Hsp72 is a functionally significant danger signal to the immune system. Cell Stress Chaperones 8, 272–286.
Concordet, J.P., Ferry, A., 1993. Physiological programmed cell death in thymocytes is induced by physical stress (exercise). Am. J. Physiol. 265, C626–C629.
Cvoro, A., Dundjerski, J., Trajkovic, D., Matic, G., 1998. Heat stress affects the glucocorticoid receptor interaction with heat shock protein Hsp70 in the rat liver. Biochem. Mol. Biol. Int. 46, 63–70.
Danese, S., Sans, M., Fiocchi, C., 2004. Inflammatory bowel disease: the role of environmental factors. Autoimmun. Rev. 3, 394–400.
Dokladny, K., Moseley, P.L., Ma, T.Y., 2006. Physiologically relevant increase in temperature causes an increase in intestinal epithelial tight junction permeability. Am. J. Physiol. Gastrointest. Liver Physiol. 290, G204–G212.
Drummond, I.A., Steinhardt, R.A., 1987. The role of oxidative stress in the induction of *Drosophila* heat-shock proteins. Exp. Cell Res. 173, 439–449.
Dutton, J., Hodgkinson, A.J., Hutchinson, G., Roberts, N.B., 1999. Evaluation of a new method for the analysis of free catecholamines in plasma using automated sample trace enrichment with dialysis and HPLC. Clin. Chem. 45, 394–399.
Dwyer, B.E., Nishimura, R.N., Brown, I.R., 1989. Synthesis of the major inducible heat shock protein in rat hippocampus after neonatal hypoxia–ischemia. Exp. Neurol. 104, 28–31.
Evdonin, A.L., Martynova, M.G., Bystrova, O.A., Guzhova, I.V., Margulis, B.A., Medvedeva, N.D., 2006. The release of Hsp70 from A431 carcinoma cells is mediated by secretory-like granules. Eur. J. Cell Biol. 85, 443–455.
Fehrenbach, E., Niess, A.M., Voelker, K., Northoff, H., Mooren, F.C., 2005. Exercise intensity and duration affect blood soluble HSP72. Int. J. Sports Med. 26, 552–557.
Fleshner, M., Campisi, J., Amiri, L., Diamond, D.M., 2004. Cat exposure induces both intra- and extracellular Hsp72: the role of adrenal hormones. Psychoneuroendocrinology 29, 1142–1152.
Fukudo, S., Abe, K., Hongo, M., Utsumi, A., Itoyama, Y., 1997. Brain–gut induction of heat shock protein (HSP) 70 mRNA by psychophysiological stress in rats. Brain Res. 757, 146–148.
Fukui, Y., Sudo, N., Yu, X.N., Nukina, H., Sogawa, H., Kubo, C., 1997. The restraint stress-induced reduction in lymphocyte cell number in lymphoid organs correlates with the suppression of in vivo antibody production. J. Neuroimmunol. 79, 211–217.
Furrie, E., Macfarlane, S., Thomson, G., Macfarlane, G.T., 2005. Toll-like receptors-2, -3 and -4 expression patterns on human colon and their regulation by mucosal-associated bacteria. Immunology 115, 565–574.
Hotchkiss, R., Nunnally, I., Lindquist, S., Taulien, J., Perdrizet, G., Karl, I., 1993. Hyperthermia protects mice against the lethal effects of endotoxin. Am. J. Physiol. 265, R1447–R1457.
Kanemi, O., Zhang, X., Sakamoto, Y., Ebina, M., Nagatomi, R., 2005. Acute stress reduces intraparenchymal lung natural killer cells via beta-adrenergic stimulation. Clin. Exp. Immunol. 139, 25–34.
Kugathasan, S.M., Sauberman, L., Smith, L., Kou, D., Itoh, J., Binion, D., Levine, A., Blumberg, R., Fiocchi, C.M., 2007. Mucosal T-cell immunoregulation varies in early and late Crohn's disease. Gut. 56, 1696–1705.
Kukreja, R.C., Kontos, M.C., Loesser, K.E., Batra, S.K., Qian, Y.Z., Gbur Jr., C.J., Naseem, S.A., Jesse, R.L., Hess, M.L., 1994. Oxidant stress increases heat shock protein 70 mRNA in isolated perfused rat heart. Am. J. Physiol. 267, H2213–H2219.
Kwon, S.B., Young, C., Kim, D.S., Choi, H.O., Kim, K.H., Chung, J.H., Eun, H.C., Park, K.C., Oh, C.K., Seo, J.S., 2002. Impaired repair ability of hsp70.1 KO mouse after UVB irradiation. J. Dermatol. Sci. 28, 144–151.
Lee, W.C., Wen, H.C., Chang, C.P., Chen, M.Y., Lin, M.T., 2006. Heat shock protein 72 overexpression protects against hyperthermia, circulatory shock, and cerebral ischemia during heatstroke. J. Appl. Physiol. 100, 2073–2082.
Levenstein, S., Prantera, C., Varvo, V., Scribano, M.L., Andreoli, A., Luzi, C., Arca, M., Berto, E., Milite, G., Marcheggiano, A., 2000. Stress and exacerbation in ulcerative colitis: a prospective study of patients enrolled in remission. Am. J. Gastroenterol. 95, 1213–1220.
Liu, T.S., Musch, M.W., Sugi, K., Walsh-Reitz, M.M., Ropeleski, M.J., Hendrickson, B.A., Pothoulakis, C., Lamont, J.T., Chang, E.B., 2003. Protective role of HSP72 against *Clostridium* difficile toxin A-induced intestinal epithelial cell dysfunction. Am. J. Physiol. Cell Physiol. 284, C1073–C1082.
Ludwig, D., Stahl, M., Ibrahim, E.T., Wenzel, B.E., Drabicki, D., Wecke, A., Fellermann, K., Stange, E.F., 1999. Enhanced intestinal expression of heat shock protein 70 in patients with inflammatory bowel diseases. Dig. Dis. Sci. 44, 1440–1447.
Mantis, N.J., Cheung, M.C., Chintalacharuvu, K.R., Rey, J., Corthesy, B., Neutra, M.R., 2002. Selective adherence of IgA to murine Peyer's patch M cells: evidence for a novel IgA receptor. J. Immunol. 169, 1844–1851.
Mawdsley, J.E., Rampton, D.S., 2005. Psychological stress in IBD: new insights into pathogenic and therapeutic implications. Gut 54, 1481–1491.
Nohta, H., Mitsui, A., Umegae, Y., Ohkura, Y., 1987. Determination of free and total catecholamines in human urine by HPLC with fluorescence detection. Biomed. Chromatogr. 2, 9–12.
Oksala, N.K., Kaarniranta, K., Tenhunen, J.J., Tiihonen, R., Heino, A., Sistonen, L., Paimela, H., Alhava, E., 2002. Reperfusion but not acute ischemia in pig small intestine induces transcriptionally mediated heat shock response in situ. Eur. Surg. Res. 34, 397–404.
Qiu, B.S., Vallance, B.A., Blennerhassett, P.A., Collins, S.M., 1999. The role of $CD4^+$ lymphocytes in the susceptibility of mice to stress-induced reactivation of experimental colitis. Nat. Med. 5, 1178–1182.
Rakoff-Nahoum, S., Paglino, J., Eslami-Varzaneh, F., Edberg, S., Medzhitov, R., 2004. Recognition of commensal microflora by Toll-like receptors is required for intestinal homeostasis. Cell 118, 229–241.
Ramaglia, V., Harapa, G.M., White, N., Buck, L.T., 2004. Bacterial infection and tissue-specific Hsp72, -73 and -90 expression in western painted turtles. Comp. Biochem. Physiol. C Toxicol. Pharmacol. 138, 139–148.
Riley, V., 1981. Psychoneuroendocrine influences on immunocompetence and neoplasia. Science 212, 1100–1109.
Rumio, C., Besusso, D., Arnaboldi, F., Palazzo, M., Selleri, S., Gariboldi, S., Akira, S., Uematsu, S., Bignami, P., Ceriani, V., Menard, S., Balsari, A., 2006. Activation of smooth muscle and myenteric plexus cells of jejunum via Toll-like receptor 4. J. Cell Physiol. 208, 47–54.
Stam, R., Akkermans, L.M., Wiegant, V.M., 1997. Trauma and the gut: interactions between stressful experience and intestinal function. Gut 40, 704–709.
Sudo, N., Yu, X.N., Sogawa, H., Kubo, C., 1997. Restraint stress causes tissue-specific changes in the immune cell distribution. Neuroimmunomodulation 4, 113–119.
Tanaka, K.I., Namba, T., Arai, Y., Fujimoto, M., Adachi, H., Sobue, G., Takeuchi, K., Nakai, A., Mizushima, T., 2007. Genetic evidence for a protective role for heat shock factor 1 and heat shock protein 70 against colitis. J. Biol. Chem. 282, 23240–23252.
Tlaskalova-Hogenova, H., Stepankova, R., Hudcovic, T., Tuckova, L., Cukrowska, B., Lodinova-Zadnikova, R., Kozakova, H., Rossmann, P., Bartova, J., Sokol, D., Funda, D.P., Borovska, D., Rehakova, Z., Sinkora, J., Hofman, J., Drastich, P., Kokesova, A., 2004. Commensal bacteria (normal microflora), mucosal immunity and chronic inflammatory and autoimmune diseases. Immunol. Lett. 93, 97–108.
Tobian, A.A., Canaday, D.H., Boom, W.H., Harding, C.V., 2004. Bacterial heat shock proteins promote CD91-dependent class I MHC cross-presentation of chaperoned peptide to $CD8^+$ T cells by cytosolic mechanisms in dendritic cells versus vacuolar mechanisms in macrophages. J. Immunol. 172, 5277–5286.
Tomasovic, S.P., Steck, P.A., Heitzman, D., 1983. Heat-stress proteins and thermal resistance in rat mammary tumor cells. Radiat. Res. 95, 399–413.
Trautinger, F., Kindas-Mugge, I., Knobler, R.M., Honigsmann, H., 1996. Stress proteins in the cellular response to ultraviolet radiation. J. Photochem. Photobiol. B 35, 141–148.
Udelsman, R., Blake, M.J., Stagg, C.A., Holbrook, N.J., 1994. Endocrine control of stress-induced heat shock protein 70 expression in vivo. Surgery 115, 611–616.
Yoneda, T., Benedetti, C., Urano, F., Clark, S.G., Harding, H.P., Ron, D., 2004. Compartment-specific perturbation of protein handling activates genes encoding mitochondrial chaperones. J. Cell Sci. 117, 4055–4066.
Yun, J.K., McCormick, T.S., Villabona, C., Judware, R.R., Espinosa, M.B., Lapetina, E.G., 1997. Inflammatory mediators are perpetuated in macrophages resistant to apoptosis induced by hypoxia. Proc. Natl. Acad. Sci. USA 94, 13903–13908.
Zhang, X., Okutsu, M., Kanemi, O., Gametchu, B., Nagatomi, R., 2005a. Repeated stress suppresses interferon-gamma production by murine intestinal intraepithelial lymphocytes. Tohoku J. Exp. Med. 206, 203–212.
Zhang, X., Okutsu, M., Kanemi, O., Nagatomi, R., 2005b. Effect of foot shock stress on the interferon-gamma production of murine intestinal intraepithelial lymphocytes. Immunol. Lett. 100, 170–176.
Zimmerman, L.H., Levine, R.A., Farber, H.W., 1991. Hypoxia induces a specific set of stress proteins in cultured endothelial cells. J. Clin. Invest. 87, 908–914.

8 摂食・嚥下リハビリテーション

Dysphagia Rehabilitation

Shin-ichi Izumi 出江 紳一
(東北大学大学院医工学研究科リハビリテーション医工学分野)
E-mail：izumis@bme.tohoku.ac.jp

Key Words
●摂食・嚥下障害
●リハビリテーション
●チーム医療
●嚥下食
●プロセスモデル

Summary

Rehabilitation for swallowing disorder was described. What is essential in dyshagia rehabilitation is care system that can provide trans-disciplinary team management. Evaluation of dysphagia includes assessment of oral hygiene, dental examination, neurological examination, physical assessment of musculoskeletal function, video-fluoroscopic examination, and video-endoscopic examination as well as evaluation of activities of daily living and quality of life. Based on findings of these tests, the route of nutrition intake is determined, such as oral intake, tube feeding, or parenteral nutrition. When oral intake is possible, specific swallowing techniques, eating postures, and food characteristics are chosen. Rehabilitation can induce re-learning of swallowing reflex and eating behaviors with preventing aspiration pneumonia and asphyxiation in patients with dysphagia, resulting in restoration of their quality of life.

著者プロフィール
出江 紳一

東北大学大学院医工学研究科リハビリテーション医工学分野教授

横浜出身。1983年 慶應義塾大学医学部卒。同助手，東海大学医学部准教授を経て，2002年 東北大学教授，2008年より現職。

東北大学教育研究評議員。リハビリテーション科専門医。第17回日本摂食・嚥下リハビリテーション学会大会長(2011年9月)。

著書に『回復する身体と脳』(中央法規出版) など。

摂食・嚥下リハビリテーションとは

摂食・嚥下リハビリテーションは単なる飲み込み訓練ではなく，さまざまな治療技術を患者の症状と環境に合わせて適用するシステムである。たとえば，日常の食事観察から嚥下障害を疑い，診察や検査に基づいて最適な摂食条件を設定し，その情報を受け取って生活の場で安全な摂食介助を行うなど，多様な専門職が勤務する部署・施設の壁を越えて連係するダイナミックな営みである。

疾患や加齢による食べることの障害に対して行われるリハビリテーションが医療技術として確立されたのはこの四半世紀である。耳鼻科領域で開発された「ビデオ嚥下造影検査」(後述) に基づいて嚥下障害の病態診断と嚥下手技や嚥下障害食による介入が発展してきた。

その目標を一言でいうと，食物移送と気道防御の再建である。両者は密接

に関連し，気道防御には適切な食物移送と気道侵入物の喀出が必要である。本稿では，この目標を達成するための評価法，ならびに治療の考え方と方法を概説する。詳細は成書[1)-5)]を参照していただきたい。

摂食・嚥下のモデル

成人の食事では，まず食物を認識し，手や食具を使って適切な量を口まで運び，捕食する。次に，咀嚼して唾液の混ざった食塊を形成しつつ，それを咽頭に送る。そこから嚥下運動が起こって食道に到達した食塊は，蠕動運動によって胃に運ばれる。この一連の行為・動作・運動は次の５期に分けられる。すなわち，先行期（何を，どのくらい，どのように食べるかを決めて口に運ぶ），準備期（捕食した食物を咀嚼する），口腔期（咀嚼された食塊を咽頭に運ぶ），咽頭期（反射運動によって咽頭から食道に食塊を運ぶ），そして食道期（蠕動運動で食塊を胃まで運ぶ）である。これは運動を生理学的に分類したモデルであり，「指示されるまで飲み込まない」嚥下（いわゆる命令嚥下）には当てはまる。一方，自然な食事では，咀嚼されている間に食物の一部は中咽頭にまで達しているのに嚥下反射は惹起されない。そこで，自然に咀嚼し嚥下する場合を考えるには，Palmer ら[6)]によって提唱された「プロセスモデル」を用いる。すなわち，「捕食から臼歯部に運ばれるまで（ステージⅠトランスポート）」，「咀嚼（プロセッシング）＋中咽頭までの移送（ステージⅡトランスポート）」，「咽頭嚥下」である。一口の捕食で通常複数回の咽頭嚥下が起こり，咽頭嚥下の直後に口腔内に残っている食塊の咀嚼と移送が再開する。

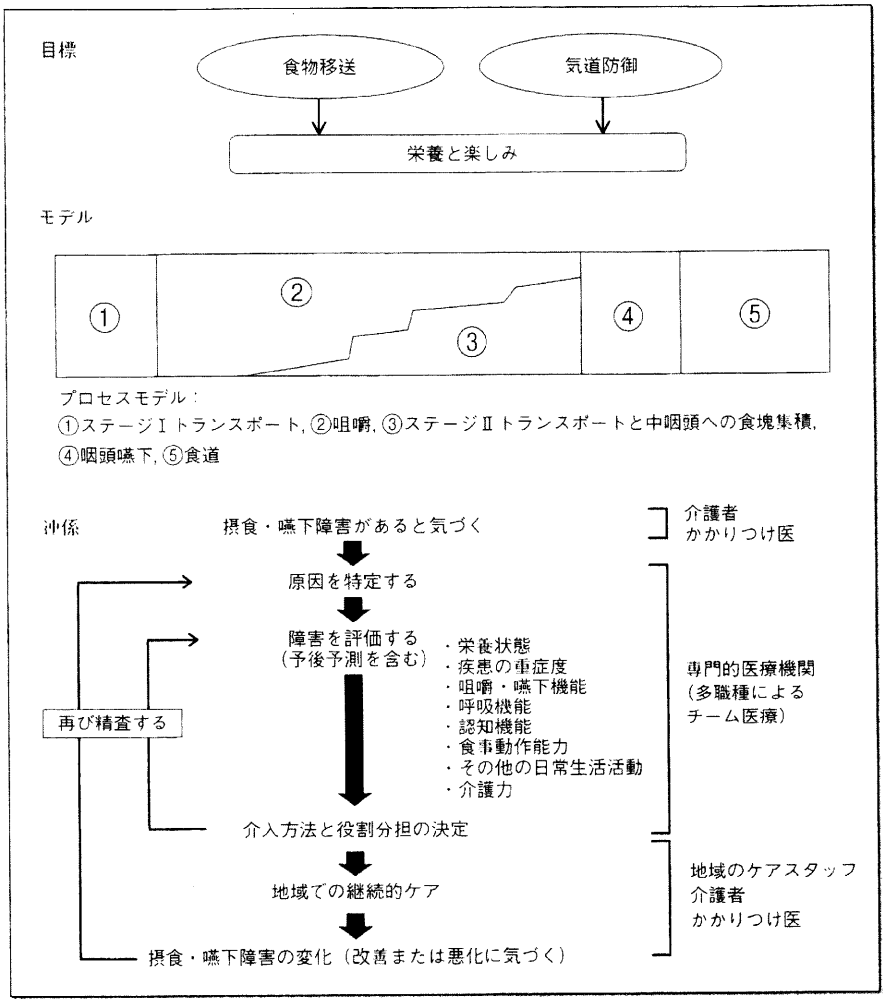

図１．概念

図１に摂食・嚥下リハビリテーションの目標，モデル，連係をまとめた。

摂食･嚥下の評価（図２）

１．口腔の観察

口腔の構造と機能，および衛生状態を観察する。たとえば，舌の萎縮の有無と運動範囲，舌苔の付着程度，現存歯数と現存歯の咬合，口腔清掃状態，口腔粘膜の乾燥の有無，分泌物の付着，口内炎の有無，軟口蓋麻痺の有無などをみる。口腔衛生の不良は味覚や触覚を鈍磨させ嚥下に悪影響を及ぼす。

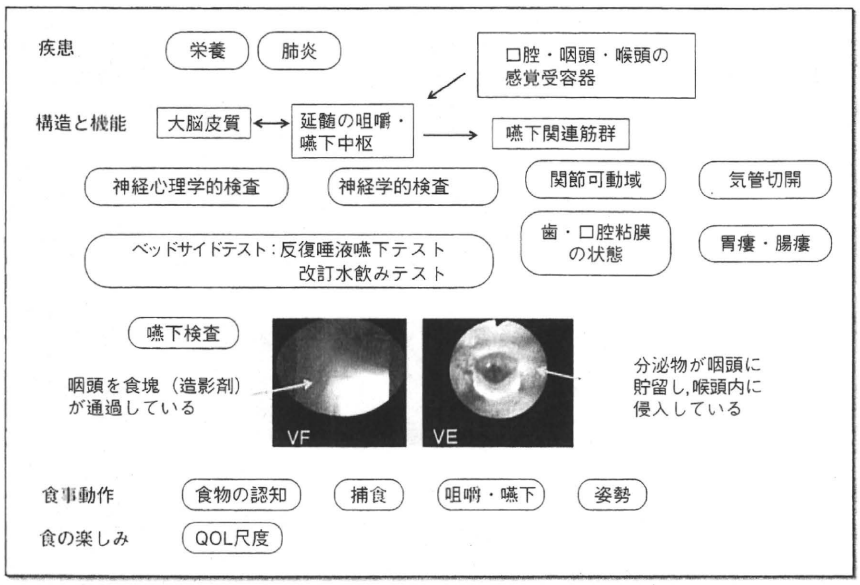

図2．診断と評価

2．食事動作の観察

安全な食事動作は，覚醒し，食物に注意が向き，食器を適切に使用し，適量の食物を口まで運び，捕食し，その間適切な姿勢を保持していることで達成される。覚醒と注意力については，声掛けへの反応と表情から判断する。上肢をうまく使えないときや一口量が多すぎるなどのときは，認知症や麻痺などの神経要因，肩関節痛などの骨関節要因，体幹傾斜などの姿勢要因，食器のデザインや食卓の高さといった環境要因などの視点から観察する。食事に長時間かかる場合には，疲労により覚醒・注意の低下や姿勢保持の困難を生じる。

3．咀嚼・嚥下の観察

食物が咀嚼されない，口の中でとどまり咽頭に送り込まれない，こぼしてしまう，嚥下反射が起こらない，むせる，鼻腔に入ってしまう，などの異常の有無や疲労の程度に加え，呼吸状態にも注意を払う。嚥下時には喉頭で気道が閉鎖され，呼吸が約１秒間停止する。これを嚥下時無呼吸という。嚥下後の咽頭に食物が残留していると，吸気から呼吸が再開された場合に誤嚥が起こることがある。

4．栄養評価

摂食・嚥下障害患者では低栄養や脱水症を生じうる。また逆に，直接的に摂食・嚥下障害を生じる疾患がない場合でも，手術後の廃用症候群のために経口摂取が困難となったり，誤嚥を生じたりすることがある。

5．嚥下検査の解釈のポイント

ベッドサイドテストとしては反復唾液嚥下テストや改訂水飲みテストがある。精査が必要な場合にはビデオ嚥下造影検査（videofluoroscopic examination of swallowing：VF）や嚥下内視鏡検査（videoendoscopic evaluation of swallowing：VE）を行う。VFでは造影剤または造影剤を混ぜた食物を摂取させる。通常は口腔から上部食道までを側方から観察するが，左右の比較をする場合には正面像をみる。VFにより造影剤の動き（誤嚥や咽頭残留の有無など）と身体（舌，軟口蓋，咽頭収縮筋，舌骨，甲状軟骨，喉頭蓋など）の動きから病態を推定する。高齢者では，頸椎の前方に突出した骨棘が誤嚥や食道入口部の通過障害を起こすことがあるので注意する。誤嚥してもむせないことをsilent aspirationという。Silent aspirationの診断にはVFが必要である。誤嚥した場合には，喉頭あるいは気道に侵入した食物を喀出することができるかどうかもみる。また，病態に合わせて水分のとろみ調節や，体幹リクライニング角度の選択，頸部回旋などの効果を検討しつつ検査を進め，誤嚥しないで摂取できる食物形態と姿勢を探索することができる。

VEではファイバースコープを鼻腔または口腔から挿入し，声門の開閉が適切になされるか，分泌物や食物が咽頭に残留したり，喉頭に侵入したりしないかを観察する。